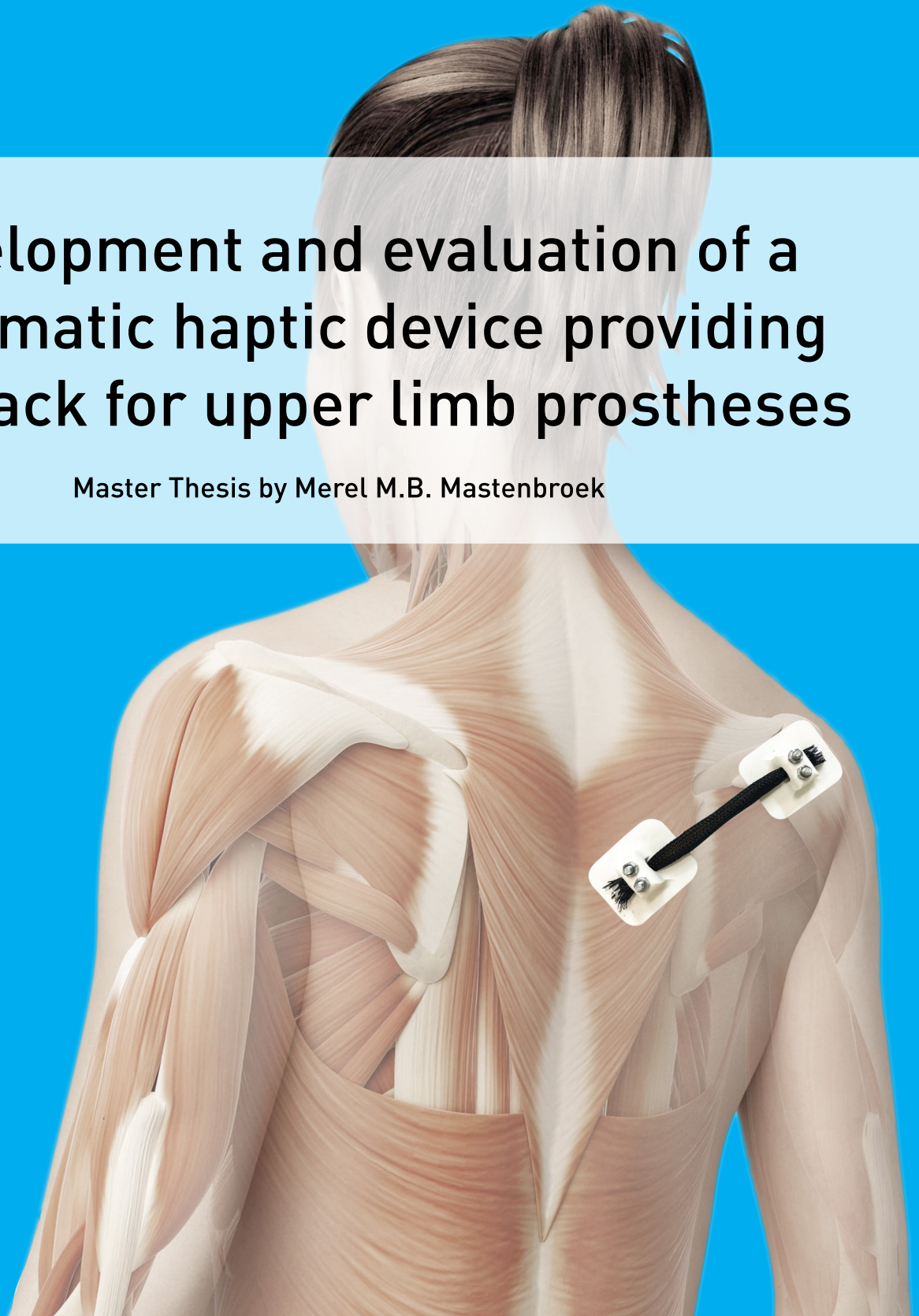


Development and evaluation of a pneumatic haptic device providing feedback for upper limb prostheses

Master Thesis by Merel M.B. Mastenbroek



Haptic feedback in upper limb prostheses

**Development and evaluation of a pneumatic
haptic device providing feedback for upper
limb prostheses.**

by

Merel Mo Brit Mastenbroek

to obtain the degree of Master of Science
at the Delft University of Technology,
to be defended on Tuesday May 11, 2021

Student number: 4723333
Project duration: July 2020 - May 2021

Thesis committee:	Prof. Dr. F. C. T. van der Helm	Chairman
	Dr. ir. D. H. Plettenburg	Daily supervisor
	Dr. T. Horeman	External committee member

An electronic version of this thesis is available at <http://repository.tudelft.nl/>.

Preface

The past years at the Delft University of Technology included hard work, a lot of fun, meeting many new people, and bursting out of my bubble in Amsterdam. I never expected to learn so much, from both the professors and also my fellow students. The transition from a Bachelor Human Movement Sciences was a large one, and during this Master's program, I really became an engineer. From programming in Matlab, to drawing in SolidWorks, to 3D-printing, to learning how to set up my own research project. I will never forget those long Multibody Dynamics days in the 'zebra-zalen', and the lectures of Medical Technology in the evenings after visiting ID Kafee.

Many people helped me during my graduation period. First, I would like to thank my supervisor Dick Plettenburg for his guidance through my literature review, internship, and final research project. It was a long period in very difficult times, but we adjusted to the situation and came up with solutions together. Secondly, I would like to thank Jan van Frankenhuyzen, who showed me everything that is possible in the Robotics Lab. No question was ever stupid and no answer was ever wrong. Building my prototype would not have been possible without him. I want to thank Jos van Driel for his guidance in finding the correct test set-up. And thanks to Frans van der Helm and Tim Horeman for being part of my graduation committee.

A special thanks to my family and friends. My parents for their unconditional love and support. They always tell me to do what makes me happy and they always support whatever decision I make. And thanks to my dad for always lending me his car whenever the NS abandoned me again. Also Anna Kay and Floris for their sharp feedback and dinner-meetings, and my other sisters for their listening to my complaining. Thanks to my high school friends in Amsterdam for their high-quality mental support, Ronald for his great feedback on my thesis. And Sanne for watching stupid TV programs together before our exams to make ourselves feel smart, and always providing me a place to stay in Delft.

*Merel Mo Brit Mastenbroek
Amsterdam, May 2021*

Abstract

Background Upper limb prostheses help people with an upper limb deficiency in performing activities of daily living. They can be divided into two categories; body-powered and externally powered prostheses. The advantage of body-powered prostheses is that they provide feedback to the user. The advantage of externally powered prostheses is the low operating force required to control the prosthesis. To reduce rejection rates of upper limb prostheses control, cosmetics and comfort should be improved. To improve control, a design was proposed integrating proprioceptive force feedback into an externally powered upper limb prosthesis with a haptic interface placed on the scapula. However, the cosmetics and comfort are to be improved. The goal of this study is to design a haptic force feedback system that meets the demands regarding comfort and cosmetics.

Method Design requirements and mechanical requirements are set. A conceptual design was made using SolidWorks and a prototype was built. The proposed prototype was tested on a test bench to evaluate the overall system. It was analyzed whether the design met the pre-set requirements and the results were compared to other devices.

Results The designed haptic device is made out of an anchoring system, pneumatic artificial muscle (PAM), and a distance sensor. The total weight of the system is 41g for the anchoring system and PAM, and 29g for the distance sensor. The dimensions are 50x25x120mm. The maximum pressure for the actuator is 3bar. The output forces reached are 87.41N, 79.04N, 100.00N, 85.38N, and 104.8N for actuators with an initial length of 80mm, 90mm, 100mm, 110mm, and 120mm respectively. The designed distance sensor measures a distance up to 58mm, with an accuracy of $\pm 1mm$. Compared to other devices the developed overall system is lighter in weight and smaller in size. Furthermore, it is made out of flexible materials, allowing the device to bend along the curve of the shoulder.

Conclusion This study presents a new design for a haptic interface to provide proprioceptive force feedback for an upper limb prosthesis. It is an improvement in cosmetics and comfort, while still meeting the mechanical requirements. Future research should be done with users of an upper limb prosthesis to evaluate the applicability.

Contents

1 Paper	1
1.1 Introduction	2
1.2 Requirements.	4
1.3 Design.	5
1.4 Testing	8
1.5 Results	9
1.6 Discussion	11
1.7 Conclusion	13
Bibliography	15
Appendices	19
A Background	21
A.1 Upper limb deficiency	21
A.2 Upper limb prostheses	21
A.2.1 Passive prostheses.	21
A.2.2 Active Prostheses	21
A.2.3 Externally powered prostheses	22
A.3 Harness system	22
A.3.1 Harness control by shoulder movements	22
A.3.2 Traditional harness design	23
A.3.3 Alternative harness design.	23
A.4 Cosmetics, comfort and control	24
A.4.1 Advantages and disadvantages	24
A.5 New designs including feedback.	25
A.6 Actuators	25
A.6.1 Piston in cylinder actuators	26
A.6.2 Rotary vane actuators	26
A.6.3 Soft pneumatic actuators.	26
A.6.4 Pneumatic Artificial Muscles	27
B Final design	29
B.1 Pneumatic artificial muscle.	29
B.2 Anchor system	31
B.3 Stringpot	33
C MATLAB code	37
C.1 Script mechanical tests muscles Force	37
C.2 Function "loopdata".	42
C.3 Script mechanical tests muscle Pressure	44
C.4 Function "pressure15N"	47
C.5 Stringpot vs laser.	48
D SOLIDWORKS Drawings	51

1

Paper

April 30, 2021

Development and evaluation of a pneumatic haptic device providing feedback for upper limb prostheses.

Merel M. B. Mastenbroek (4723333)

1.1. Introduction

Upper limb deficiency is a condition in which a part of the upper limb is missing, caused by a congenital defect, an acquired defect, or trauma. Studies show a prevalence of 0.8 per 10.000 inhabitants in The Netherlands and 1.4 per 10.000 inhabitants in the United States of America [1, 2]. Arm prostheses are important to enable optimal functional rehabilitation for people with an upper limb deficiency. These prostheses can support a patient greatly in performing activities of daily living (ADL). Despite many studies that tried to enhance the prosthetic design, rejection rates vary between 23%-45%. These rejection rates are mostly caused by not meeting the demands of users regarding cosmetics, comfort, and control of the prosthesis. Users want a prosthesis to be comfortable to wear, aesthetically pleasing, and easy to control [3, 4]. The different kind of prostheses for the upper limb all have their own advantages and disadvantages when it comes to the demands of the users.

Prostheses for the upper limb can be divided into categories [5]:

- Passive prostheses: Require external control and activation of the prosthetic hand/ tool.
 - Prosthetic hands: an aesthetic replacement of the missing hand.
 - Prosthetic tools: used for specific tasks.
- Active prostheses: Require internal control and activation of the prosthetic hand.
 - Body powered (BP) prostheses: driven by movements of the user's body.
 - Externally powered (EP) prostheses: powered by an external source (e.g. hydraulic, electric or pneumatic actuator).

Body-powered (BP) prostheses are often actuated by pulling a Bowden cable, which is attached to the user's shoulder with a harness.

Moving the shoulder forward and backward, or extending and flexing the arm attached to the prosthesis will open and close the prosthetic hand. This requires cable operation forces that range between 33 and 131 Newton (N) to achieve a pinch force of 15 N , the mean pinch force in ADL. These forces cause fatigue and result in high prostheses rejection rates [3]. To achieve fatigue-free operation of a BP prosthesis, the operating force of the cable should be a maximum of 38 N for women and 66 N for men [6]. The main advantage of BP prostheses is the feedback provided back to the user by the Bowden cable; the user can feel the amount of input force needed to pull the cable, providing information about the control of the prosthesis.

Externally powered prostheses do not have this disadvantage of high actuation forces, since the actuation is derived from an external power source. The actuation can for example be electric, hydraulic (driven by fluids), or pneumatic (driven by compressed air). No high actuation forces of the user are needed. However, there is no proprioceptive feedback regarding the opening width, the applied pinch force, or external forces. The user has to rely on only visual and auditory feedback of the prosthesis [3]. The absence of proprioceptive force feedback in externally powered prosthesis has a negative impact on the control of the prosthesis. It requires a higher mental load to control, compared to BP prostheses that are regarded more intuitive in control [7].

Vardy et al. (2017) proposed a concept of an upper limb prosthesis with the best of both worlds; an externally powered prosthesis that is able to provide proprioceptive feedback through a haptic interface [7]. This haptic interface provides force feedback in the same location as BP prostheses; it is placed on the shoulder (the shoulder blade, or scapula) using an anchor system consisting of two skin anchors, see Figure 1.1.

Moving the shoulder generates an actuation force between the two skin anchors on the scapula. This force is measured and is sent wirelessly to the prosthetic hand, which in response opens or

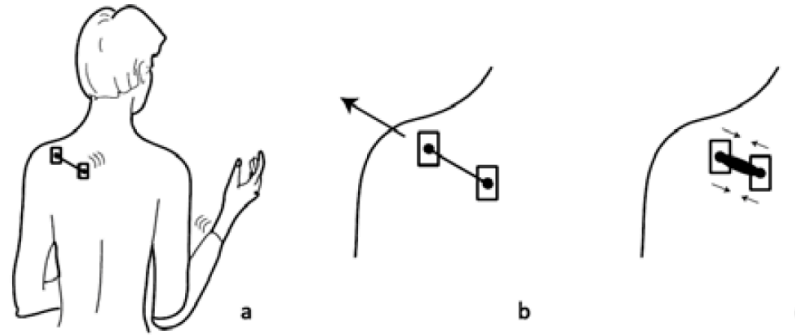


Figure 1.1: The proposed design of the haptic interface by Vardy et al. (2017). (a) The skin anchors placed on the scapula with wireless connection to the prosthetic hand, (b) movement of the shoulder changes the force between the two skin anchors which opens or closes the prosthetic hand, (c) proprioceptive feedback is fed back to the user by pulling the skin anchors closer together, as a result of an external force on the prosthetic hand. The figure is retrieved from [7].

closes. Oppositely, an external perturbation force acting on the prosthetic hand will be fed back to the haptic system on the scapula. An actuator pulls the two skin anchors closer together as shown in Figure 1.1c. Pulling the skin anchors together provides a force on the scapula of the user as proprioceptive force feedback.

A study by J. Lambers (2019) continued on the system of Vardy et al. (2017). Whereas Vardy et al. [7] measured the force between the skin anchors on the scapula as input, J. Lambers [8] measured the distance between the skin anchors as input. In both studies, the proprioceptive feedback was provided by pulling the skin anchors on the scapula together. The skin anchors in the study of Vardy et al. [7] were pulled together by an electrical actuator, the system of J. Lambers [8] included a pneumatic actuator, see Figure 1.3. Pneumatic actuators are suitable for this type of prosthesis and feedback design since they are lightweight, safe, compact, fast, easy to install and they require overall low maintenance [9–11]. Although electric actuators are more accurate than pneumatic actuators, the study of J. Lambers showed that the accuracy of a pneumatic actuator was high enough for this haptic feedback design [8].

Figure 1.3 shows the haptic device of the study of J. Lambers [8]. It includes a pneumatic cylinder as an actuator to provide the proprioceptive force feedback, indicated by number 1 in the figure. Secondly, it includes a pneumatic valve to control the pneumatic actuator, indicated by number 3. It also includes a laser sensor to measure the distance between the skin anchors, indicated by number 2. A control diagram of the system is shown in Figure 1.2.

Both the laser sensor and the pneumatic cylinder

are not able to bend along the curvature of the shoulder. To compensate for the curvature of the shoulder and keep the system in a straight line, a hinge system was included. As a result, the whole system turned out quite large. The dimensions are 155x85x50 millimeters (mm) and it weighs 272 grams (g). The large dimensions and weight of the system are perceived as inconvenient and heavy. Besides this, J. Lambers attached the system to the scapula of the participants using regular tape, which was not considered a long-term solution [8].

This study is a continuation of the study done by J. Lambers [8], which provided a proof of principle of the pneumatically actuated haptic system. A wearable design is yet to be made and cosmetics and comfort can be improved. The cosmetic value of a prosthesis increases with reducing wear and tear of the design. To reach a high cosmetic value, a small, lightweight, smooth-edged design is favoured. To reach a high value of comfort, a lightweight design with body-adapted small area fittings is preferred [12].

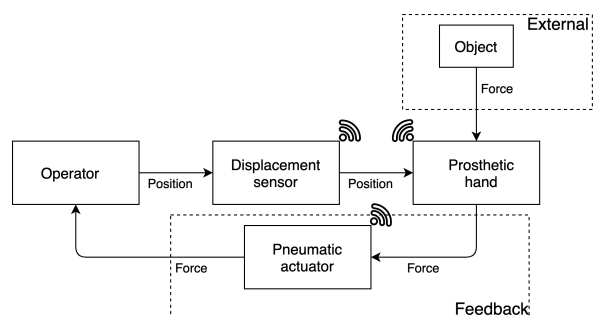


Figure 1.2: Control diagram of the system of J. Lambers (2019).

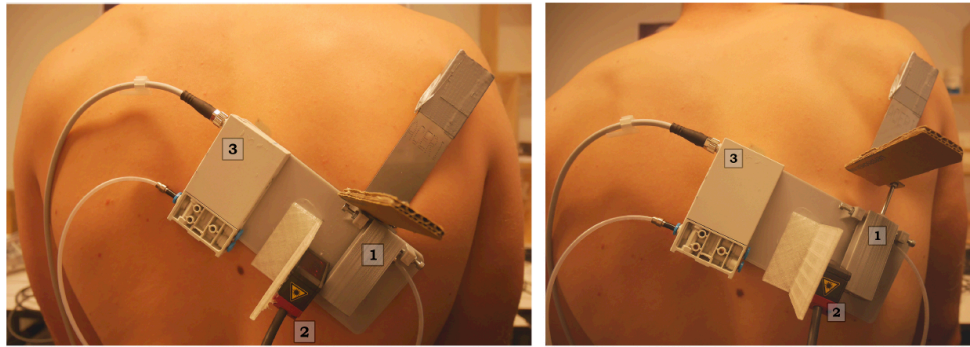


Figure 1.3: The pneumatic feedback system of Lambers (2019) [8]. This includes (1) a pneumatic cylinder, (2) a laser sensor and (3) a pneumatic valve. Left: The system with the shoulder in normal position. Right: The system with the shoulder in protracted/elevated position.

Problem definition

To reduce rejection rates of upper limb prostheses, the control, cosmetics, and comfort should be improved. Providing the user with force feedback enhances the control of a prosthesis [3, 13]. Vardy et al. (2017) proposed a design including a haptic interface that provides proprioceptive force feedback [7]. This design of an upper limb prosthesis does not have a cable or high cable operation forces and still provides force feedback to its user. A proof of principle has been done by J. Lambers [8]. However, regarding cosmetics and comfort, there is room for improvement. The system of J. Lambers has a weight of 272g, which makes it unsuitable to wear all day. Besides that, it is considerably large in size, with dimensions of 155x85x50mm. This makes the system inadequate to be worn underneath clothing. Moreover, the system is unable to bend with the curvature of a scapula because of the laser sensor and the pneumatic cylinder, resulting in the addition of the hinge system. And finally, J. Lambers used tape to attach the system to the scapula.

Goal

The goal of this study is to design and evaluate a pneumatic haptic interface device for an upper limb prosthesis that fulfills user demands regarding cosmetics and comfort. The design has to be lightweight, small, and smooth-edged with body-adapted small area fittings, and still meet the pre-set mechanical requirements.

Outline

This paper will start with the requirements in Chapter 1.2. Then, a detailed description of the design and methods of the system will be explained in Chapter 1.3. In Chapter 1.4 the mechanical tests are explained, showing the

results in Chapter 1.5. Finally, the design and results will be discussed in Chapter 1.6 and Chapter 1.7 provides the conclusion of this study.

1.2. Requirements

Before a design is made, the design requirements have to be set. To improve the cosmetics and comfort of the device, requirements regarding weight, size, and amount of force were set. The feasibility study of J. Lambers [8] showed the possibilities of a pneumatic haptic device, so equal requirements were applied to compare the devices with each other. An overview of the requirements can be found in Figure 1.4.

Overall system

To optimize the comfort of the device, the weight should be as low as possible. The device of Lambers weighed 272 grams (g) [8]. Additionally, the whole system should be small to fit underneath clothing. The dimensions of the device of J. Lambers are 155x85x50 millimeters (mm). The design includes a pneumatic cylinder, which is a rigid, hard device. Moreover, to compensate for the curvature of the shoulder, a hinge system was included, resulting in a large, inflexible system. The design of this system should be made without the hinge system to compensate for the curvature of the shoulder. The weight should be preferably below 272g, and the dimensions should be smaller than 155x85x50mm.

Actuator

The actuator provides the feedback by pulling two skin anchors closer together. It would be advantageous to take the two points for the skin anchors between which the change in distance is large, so the resolution to control the position is

opportune. Vardy & Plettenburg (2014) researched the largest displacements between two points on the scapula that could be reached [14]. The motion of 26 points was analyzed during 5 different shoulder motions; elevation, depression, protraction, retraction, and a combination of elevation and protraction. It appeared that elevation and protraction resulted in the largest change in distance with a medium change of 34mm [14]. This means that the stroke of the actuator (the distance traveled by an actuator) should be around 34mm as well. The actuator should be flexible to bend along the shoulder during these elevation/ depression/ protraction/ retraction movements. Regarding operation forces, Vardy et al. (2017) state that static forces below 2N are considered too low, and a maximum force of 10N is considered comfortable and will not cause fatigue [7]. Plettenburg et al. (2011) stated that optimal cable operation forces for body-powered prostheses were found between 10N and 20N [7, 13]. Taking comfort into account, a limited force of 15N is considered a reasonable maximum to avoid fatigue and improve comfort. The actuator needs to reach these forces.

Anchor system

The anchor system provides the attachment of the pneumatic actuator to the skin of the user in the scapular region. Since it is placed directly onto the skin it should have a smooth surface on the bottom. It needs to be lightweight and curve along the shape of the shoulder to improve the comfort. Also, it needs to be wearable underneath clothing and thus be small in size and have a smooth surface so it does not damage any clothing. Therefore, it should not include any rough edges.

Distance sensor

The distance measurement sensor has to measure the distance between two points on the scapula, to provide input for the prosthetic hand. J. Lambers used a laser sensor to do this, but this includes some disadvantages. A laser sends out a pulse of light and detects the reflection. So firstly, this implies that the path of this pulse of light needs to be straight, otherwise the reflection will divert out of range. Secondly, there needs to be an extra object for the pulse of light to reflect on. Moreover, this device is meant to be worn on the scapula underneath clothing. A laser sensor will not work in this case, since the laser will not have a clear path. The average change in distance the shoulder can generate is 34mm , so

the device needs to be at least capable of reaching these values.

	Required	Preferred
Entire system	- Weight: $< 272\text{ gr}$ - Size: $< 155 \times 85 \times 50\text{ mm}$	- No hinge system
Actuator	- Force: $> 15\text{ N}$ - Stroke: 34 mm - Pneumatic	- Flexible - Soft
Anchor system	- Human friendly	- Small - Smooth edges
Distance measurement	- Range: change in distance of $> 34\text{ mm}$	- Bend with curve of shoulder

Figure 1.4: Table of the design requirements. A distinction is made between what is required and preferred.

1.3. Design

The design of the overall device can be divided into three parts; the design of the pneumatic actuator, the design of the skin anchor system, and the design of the distance measurement sensor. In this paragraph, the chosen solutions are explained in more detail.

Pneumatic actuator design

Pneumatic actuators are lightweight, have a good energy-to-weight and force-to-weight relationship, and are quick, which makes them suitable for this design [15, 16]. Moreover, they can be made out of soft, flexible materials. To improve wearability and comfortability of this haptic system, this design includes a pneumatic artificial muscle (PAM). PAMs are pneumatic actuators that consist of an inner bladder (or balloon) and outer mesh. When compressed air is let into the bladder it pushes to the outer mesh. This converts the increase in diameter into a shortening of the actuator and a pulling force is generated.

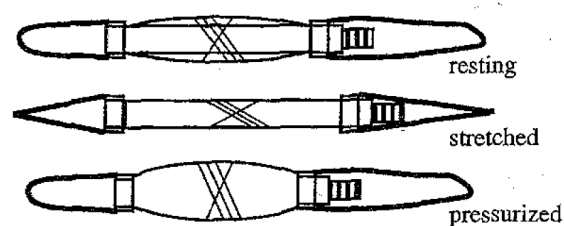


Figure 1.5: Schematic drawings of a PAM. The threads of the outer shell translate the increase in diameter into a decrease in length of the muscle. Retrieved from [17].

The shortening of a PAM is also referred to as the contraction. This can be described as the percentage of the length of the muscle (L) in relation to its initial length (L_0).

$$contraction(\%) = \frac{L}{L_0} * 100\%$$

A PAM can be made out of soft materials, and a PAM can bend along the curvature of the shoulder. It was decided to design a PAM, that could be easily made and would be flexible to bend along with the movements of the shoulder. The final design of the PAM consists of an inner balloon, outer shell, and two end parts of which one has a connection for compressed air, see Figure 1.6. It is important to select the right inner balloon. It had to be small in diameter to keep the dimensions of the design limited, of thin material, but strong enough to handle the required pressure. It appeared that modeling balloons (balloons often used to fold into animals or other figures) were suitable for this design. The outer layer needs to have threads woven in such a direction that an expansion of the diameter of the balloon when blown up results in a shortening, see Figure 1.5. A cable sleeve has these properties and was chosen as the material for the outer layer.

Two end parts were designed to attach the balloon and outer layer on. One of the endings includes an M3 screw thread for the connection of the compressed air and is hollow from the inside to allow the air to pass through. They both have ridges so the balloon would not slide off with increasing pressure. They were made out of aluminum, a strong and light material. The parts are 23mm long, the thick end is 10mm in diameter and the small end is 5mm in diameter. To ensure the attachment of the balloon to the endings and minimize air leakage, heat shrink tubing was added. To clamp everything together, U-bolts were used.

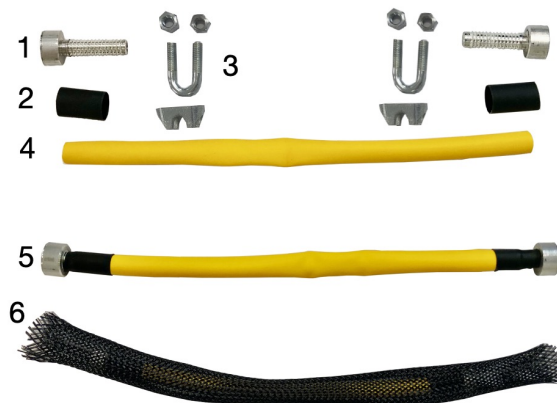


Figure 1.6: Parts to make a PAM: (1) designed end-part (2) heat shrink (3) U-bolt, (4) balloon, (5) balloon attached to the endings, and (6) the outer shell (cable sleeve) wrapped around the balloon and its endings.

The length of the muscle could easily be varied. The initial design had a length of 120mm since the assumption is that the muscle contracts up to 25% to 30% of its initial length and a stroke of 34mm will be reached. This was based on the fact that a pneumatic muscle made by the Shadow Robot Company had a contraction rate of that value [18].

Anchor system design

To attach the pneumatic actuator to the scapula, an anchor system is needed. Debra Latour invented a system for body-powered prostheses, named the Ipsilateral Scapular Cutaneous Anchor System [19]. This design was the first to remove the harness from BP prostheses and included a sticker to attach the Bowden cable to. The design of D. Latour was used as inspiration, and adjusted to fit into this system with the pneumatic actuator. The final design consists of two 3D-printed skin anchors that can be attached to the skin of the shoulder with skin-friendly tape (for example wig-tape). The skin anchors were designed in such a way that the pneumatic muscle with U-bolts fit perfectly. The anchors are 50mm wide, 60mm long, and 17mm high, with the flat bottom part at 0.5mm thickness. The anchors were 3D printed using the Ultimaker S3 printer, with MakerPoint Flex 45 material and polyvinyl alcohol support material (PVA). MakerPoint Flex material creates a flexible rubber while printing a thin layer of material, which is ideal since it will be attached to the skin of the user. Flexible material can move along with the deformations of the skin, making it more comfortable. The U-shaped part of the U-bolt is attached from the bottom and tightened at the top with bolts. A 3D model of the skin anchor was created in SolidWorks and can be found in Figure 1.7.

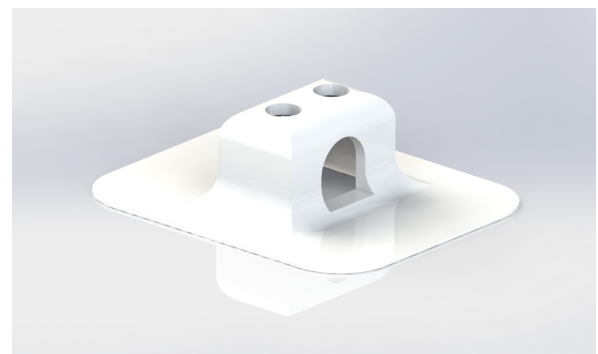


Figure 1.7: 3D-render of the designed skin anchor.

More detailed 3D-models of the pneumatic muscle and the anchor system can be found in

Appendix B. The technical drawings can be found in Appendix D. The figures below show the pneumatic muscle (PAM) attached to the anchor system and a 3D-model showing the exploded view of the overall system.



Figure 1.8: An assembled version of the developed pneumatic muscle (PAM) and skin anchor system.

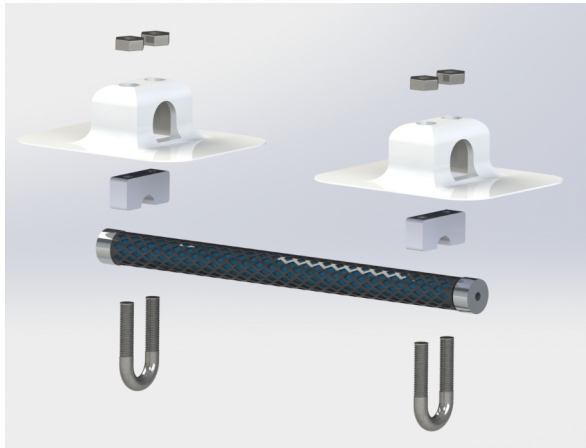


Figure 1.9: An exploded view of a 3D-render of a pneumatic muscle (PAM) and skin anchor system.

Distance sensor

To measure the distance, a version of a string potentiometer, also referred to as a draw wire sensor or a stringpot, was made. A string potentiometer is a wire actuated position sensor that measures linear distance with a cable and a spring-loaded spool.

For this design, a small, simplified and cheap version was developed. This was done by attaching a potentiometer to a spring-activated key-retractor. By pulling the cable, the inside mechanism of the key-retractor will turn, and with that the attached rotary potentiometer. The output signal of the potentiometer (the angle of the potentiometer, which is a value between 0 and 1023) can be translated to the distance covered by the wire. The stringpot had to bridge the distance of 34mm. The wire of the key-retractor was wrapped around a plastic circle attached to a spring with a diameter of 25mm. If one full turn was utilized, a maximum distance of $25mm * \pi = 78.54mm$ could be reached, which should cover enough change in distance.

However, most single-turn rotary potentiometers do not use a full range of 360° . The potentiometer that was used is a single turn precision rotary potentiometer with a range of 275° . Thus, the distance that could be measured was:

$$\frac{25 * \pi}{360} * 275 = 60mm$$

To attach the potentiometer to the turning mechanism of the key-retractor, an attachment piece and a box were designed. They were designed in SolidWorks and printed with an Ultimaker 3D printer from tough polylactic acid (PLA) black material and polyvinyl alcohol (PVA) as support material. The attachment piece was designed to fit onto the turning spring mechanism of the key-retractor. The rotational part of the potentiometer had to fit onto the key-retractor in such a way that the turning mechanism of the key-retractor creates a turning movement of the potentiometer. The box was designed to fit the key-retractor and the attachment piece into it. The lid of the box prevents the top part of the potentiometer from turning, to ensure only the required part can turn. The exact dimensions of all the parts can be found in the technical drawings in Appendix D.

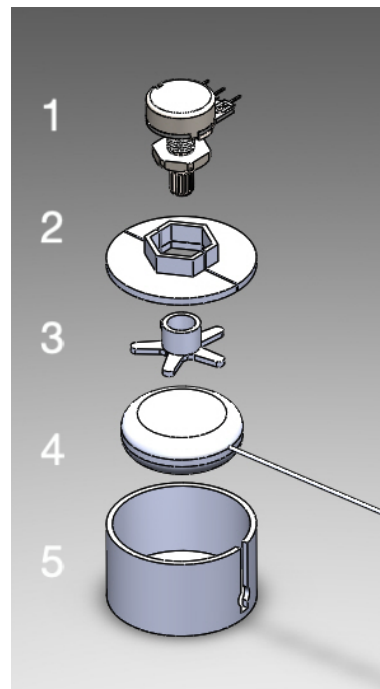


Figure 1.10: Exploded view of the developed distance sensor (the stringpot); (1) potentiometer, (2) lid, (3) attachment piece, (4) key-retractor (schematic drawing), (5) box.



Figure 1.11: All parts of the stringpot. From left to right: Box, key-retractor, lit, potentiometer with attachment piece.

Calibration

To calibrate the potentiometer and to calculate the distance, the potentiometer was connected to an Arduino UNO. The Arduino was connected to a laptop, which was also its power source, and it read the output signal of the potentiometer. Multiple tests were executed where the value of the potentiometer was read and the distance of the wire measured. These results were plotted and a function was fit between the data points using MATLAB. This function was imported into the Arduino code, so the sensor value would directly be computed into the distance covered by the wire.

1.4. Testing

Mechanical tests were performed to evaluate the properties of the designed system and to test whether the system meets the in Chapter 1.2 mentioned requirements.

First, a test was performed to find the maximum pressure a pneumatic muscle (PAM) could handle and it snapped at 3.5bar . To keep the tests safe, and the muscles intact, the maximum pressure was considered to be at 3bar . This is comparable to the pneumatic muscles created by the Shadow Robot Company [18].

During the testing, the following was measured:

1. The dimensions and weight of the parts and overall system.
2. The output force of PAMs with varying initial length (L_0) at a pressure of 3bar at different lengths of that muscle.
3. The pressure needed for PAMs with varying L_0 to reach an output force of 15N at different lengths of that muscle.
4. The output force of PAMs with varying L_0 , at initial length, at a pressure of 3bar , over a time period of 3 minutes.
5. The distance measured by the stringpot next to the distance measured by the laser sensor.

First, the size of all the parts was measured using a caliper, and the weight was determined with a regular scale.

The second test was performed to assess the output force a PAM could produce at maximum pressure. Also, the impact of a shorter or longer initial length of a PAM could be determined and the force gradient of a muscle while it contracts. The third test was done to determine the required pressure to reach an output force of 15N . PAMs with varying L_0 were tested and they were held at different lengths/ contraction percentages. The fourth test involved measuring the effect the pressure would have on the balloon of the PAM. Since it is a viscous material, it could result in deformations, and it was important to clarify whether this would affect the output force the PAMs produce.

Finally, the distance the developed stringpot measured was compared to that of a laser sensor to determine the accuracy of the stringpot distance sensor.

Test setup

The test setup to test the mechanical properties of the developed PAMs included a laser sensor, FUTEK miniature s-beam load cell (LSB200) [20], compressed air tank, Thermo Teknik pressure sensor (0-10bar), SCAIME analog signal conditioner (CPJ-CPJ2S) [21], National Instruments data acquisition system (USB6211) [22], laptop with LabView 2018, fabricated system to hold the developed PAM in place, and a turning wheel to shorten/ lengthen the PAM. A schematic overview of the setup can be found in Figure 1.12. The laser sensor was placed next to the pneumatic muscle and measured its length. The signal was sent to an amplifier and the data acquisition system of National Instruments. The load cell was placed between the PAM and the spindle and measured the pulling output force of the PAMs. The pressure sensor measured the pressure of the compressed air that was let into the PAMs. All the data was gathered and saved on a laptop using LabView 2018.

Output force

To measure the output force a muscle could generate at different lengths (in other words the different contraction percentages), the pneumatic muscle was anchored at one end, and the other end was attached to a load cell and a turning spindle. In this way, the length of the pneumatic muscle could be fixed. Every test started at the initial length (L_0) of the muscle. The pressure was increased up to 3bar , and the output force

was measured by the FUTEK load cell. The laser sensor was placed at one end of the muscle. It measured the distance (thus the length of the muscle) and had to reverberate onto a surface, so a small surface was attached to the other end of the muscle for the laser to reflect on. The muscle would then be shortened $5mm$, by turning the spindle, and the output force was measured again. This was done until the minimum length of the muscle (or maximum contraction) was reached. Muscles with a varying L_0 of $120mm$, $110mm$, $100mm$, $90mm$, and $80mm$ were tested. Every test was performed three times.

Pressure for 15N

The second test measured the required pressure of the compressed air to reach an output force of $15N$. Comparable to the test mentioned before, the PAM started at its initial length and was decreased with steps of $5mm$ until the minimum length (or maximum contraction) was reached. At every different length of the PAM, the pressure was adjusted and measured until the output force of $15N$ was reached.

Output force over 3 minutes

The third test included measuring the output force of a PAM over a time period of three minutes. To achieve this, the PAM was fixed at its initial length at a pressure of $3bar$. The output force and length were measured continuously.

Output of the stringpot

Finally, the output of the developed stringpot and laser sensor was measured. For this test,

another setup was used, see Figure 1.13. The two distance sensors were placed next to each other. The wire of the stringpot was attached to the same surface the laser bounced onto. The output of the laser was sent to the laptop with LabView, while the signal of the stringpot was read by the Arduino and sent to the laptop's Arduino program. In MATLAB the output signals were compared to each other.

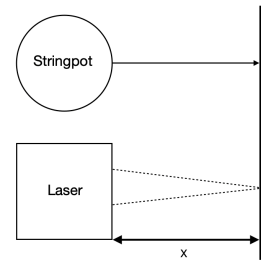


Figure 1.13: Setup for the test comparing the developed distance sensor (stringpot) next to a laser sensor. The measured distance (x) to a surface.

1.5. Results

Before the mechanical tests were performed, the weight and dimensions of the system were determined. The results can be seen in the table below (1.14). Adding the weight of a PAM with a L_0 of $120mm$ with the U-bolts and two skin anchors together results in a total weight of $41 + 29 + 1.5 = 71.5g$.

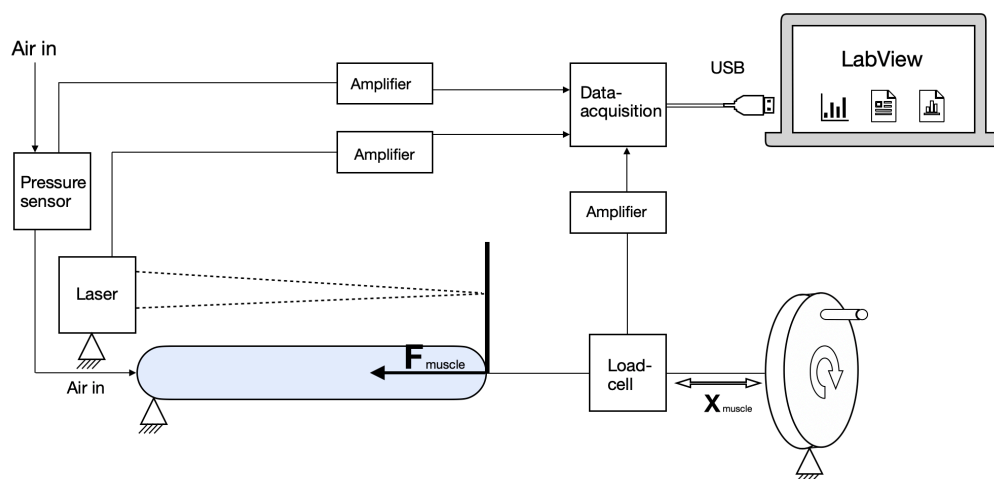


Figure 1.12: Schematic overview of the test setup. One end of the PAM is fixed, and via a load cell attached to a turning spindle. When the spindle turns, the length of the PAM (x_{muscle}) shortens/ lengthens. The laser sensor measures the length of the PAM. The pressure sensor measures the pressure of the air let into the PAM. All data is sent to the data acquisition, and the laptop.

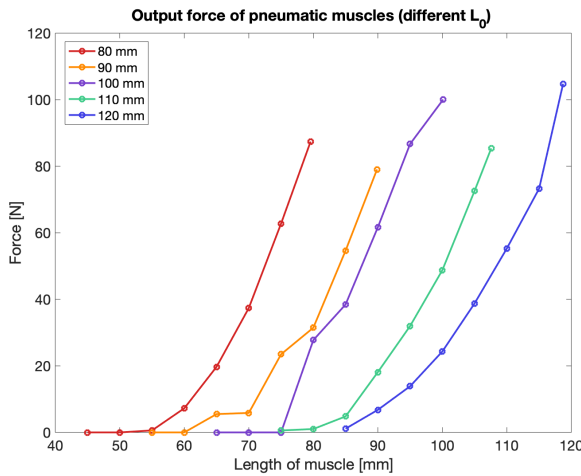
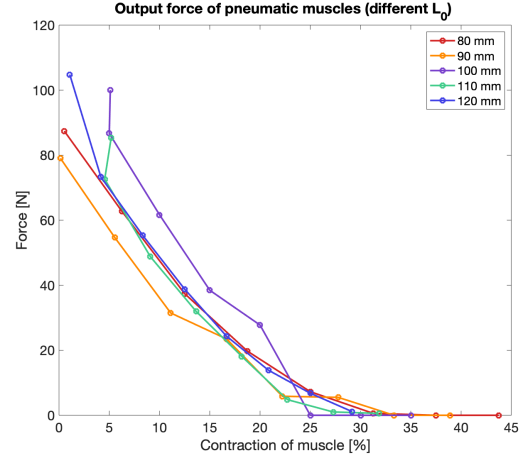
	Dimensions	Weight
Muscle	$\varnothing = 10$ mm Length = variable	5 - 8 g (depends on length)
Skin anchor	50x60x17 mm	4 g
Muscle + anchor system	Width = 50 mm Length = variable Height = 25 mm	PAM 8 g
		2 clamps 25 g
		2 anchors 8 g
		total 41 g
Stringpot	$\varnothing = 34$ mm Height = 41 mm	29 g
Stringpot anchor	50x60x6 mm	1.5 g
Total	Width = 50 mm Length = variable Height = 41 mm	71.5 g

Figure 1.14: Table of weight and size of the different parts.

The second test performed, included finding the maximum pressure the pneumatic muscles could withstand. It appeared that the muscles snapped between the 3.5 and 4 bar. As a result, we considered the maximum pressure of 3 bar for the following tests.

Output force

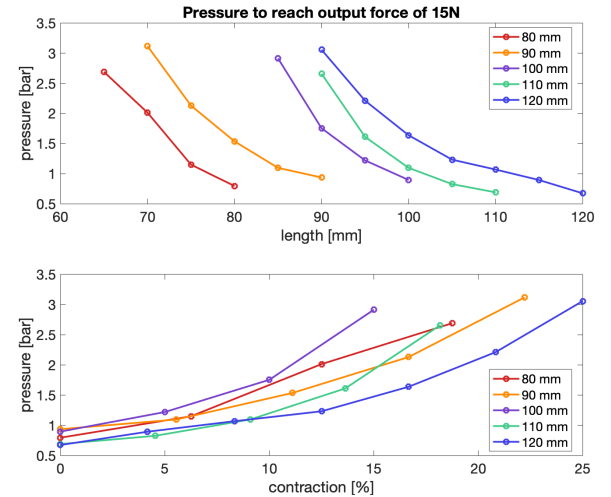
The results of the first mechanical test, which included testing the forces of pneumatic muscles with varying L_0 can be seen in Figures 1.15 and 1.16. The first figure (1.15) shows the force in relation to the length in mm of the pneumatic muscles. The second figure shows the measured output force with respect to the contraction rate of the pneumatic muscles. The maximum output force is 87.41N, 79.04N, 100.00N, 85.38N, and 104.8N for muscles with a L_0 of 80mm, 90mm, 100mm, 110mm, and 120mm respectively.

Figure 1.15: Force-length relationship of pneumatic muscles with a L_0 of 80mm, 90mm, 100mm, 110mm, and 120mm.Figure 1.16: Force-contraction relationship of pneumatic muscles with a L_0 of 80mm, 90mm, 100mm, 110mm, and 120mm.

The contraction percentage the PAMs reach are between 25% and 30%. This means that the maximum stroke of the muscles was between 20 – 24mm, 22.5 – 27mm, 25 – 30mm, 27.5 – 33mm, and 30 – 36mm for the muscles with L_0 of 80mm, 90mm, 100mm, 110mm, and 120mm respectively.

Pressure for 15N output force

The results of the test measuring the pressure required to reach an output force of 15N can be seen in Figure 1.17. This test was performed on all muscles with varying initial lengths ranging from 80mm to 120mm.

Figure 1.17: Pressure required to reach an output force of 15N. For muscles with a L_0 of 80mm, 90mm, 100mm, 110mm, and 120mm. Upper image; in relation to the length of a PAM. Lower image; in relation to the contraction percentage.

Output force over 3min

The third test, measuring the output force over a 3min time period at a pressure of 3bar , showed a decrease in force. The muscles all showed a decrease in force of (mean \pm std) $2.1 \pm 0.99\text{N}$.

Output of the stringpot

The stringpot was placed next to a laser, and both distance measurements can be seen in Figure 1.18. Three tests were performed. In the boxplot, Figure 1.19, the mean difference in the measured distance by the laser and stringpot, and the standard deviation of the difference is plotted. The results for each test are shown.

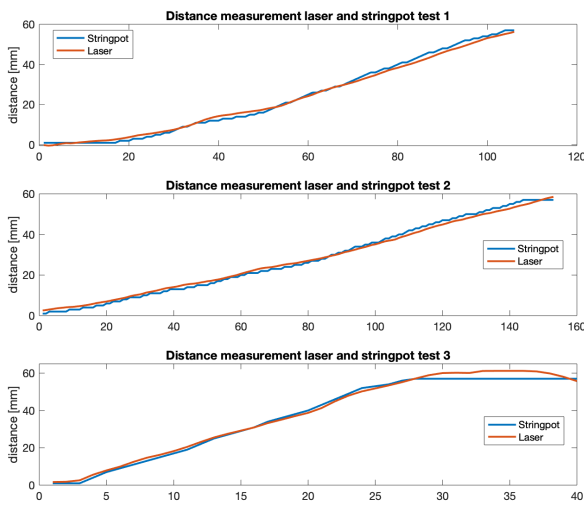


Figure 1.18: Distance measurement of a laser and the stringpot plotted in the same figure. Each figure is a different test.

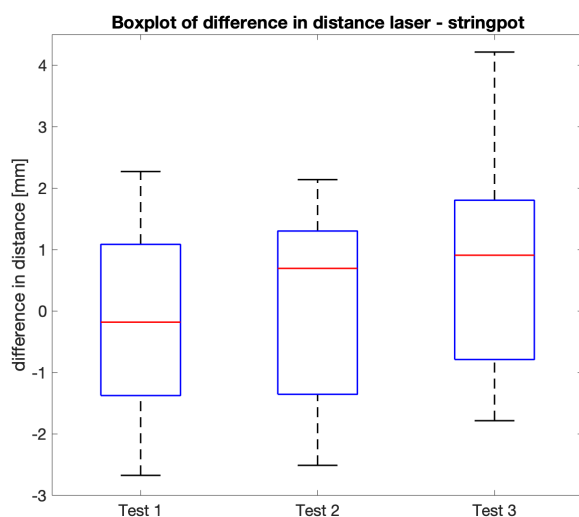


Figure 1.19: Boxplot showing the difference in measured distance between the laser and stringpot in mm. Showing the mean value (red line) and the standard deviation (blue lines).

1.6. Discussion

This study comprises the development of a haptic device, which includes an actuator (the PAM), an anchor system, and a distance sensor (the stringpot). In this section, the results of the overall system will be discussed and compared to the set requirements. By then comparing the different systems, recommendations for further development of this system and future research will be given.

Overall system

The weight and dimensions of the final design are shown in table 1.14. A total weight of 71.5g is substantially lower compared to the requirement, which was 272g . The overall system dimensions of 50mm wide and 25mm high and a variable length (depending on the chosen PAM length) between 80mm and 120mm are considerably smaller than the pre-set requirement of $155 \times 85 \times 50\text{mm}$. Regarding the dimensions, the preferred height requirement of the system was set at 25mm to improve the systems fit underneath clothing. The most ideal system is as flat as possible. The PAM and anchor system together are 25mm high, whereas the stringpot is a bit higher compared to the requirement with its height of 41mm .

Anchor system

To attach the system to the skin of the user, the anchor has to be comfortable. Therefore, the preferred requirement regarding the anchor system was set to be small and with smooth edges and it had to be human friendly. The skin anchors are developed using a 3D printer, which allows adjusting the dimensions to personal preferences. The skin anchors can easily be attached to the skin in the shoulder area with skin-friendly tape (for example wig tape), making it a human-friendly design. The attachment of the actuator to the anchor system makes use of U-bolts, that stick out through the skin anchors which could damage clothing. In the future, these tops should be covered, which could be done with caps or tape. The skin anchors are small in size and have a weight of 8g , which contributes to a comfortable overall system.

Actuator

A flexible pneumatic artificial muscle (PAM) is developed. The mechanical requirements regarding the pneumatic actuator were set at an output force of 15N to keep the forces low and a stroke of 34mm to reach the average

displacement of a shoulder. In Figure 1.15 it can be seen that the maximum forces are $87.41N$, $79.04N$, $100.00N$, $85.38N$, and $104.8N$. The figure shows that the output forces decrease when the contraction percentage increases, showing a non-linear force-contraction relationship. This was also found in other studies, see Figure 1.20 [11, 23].

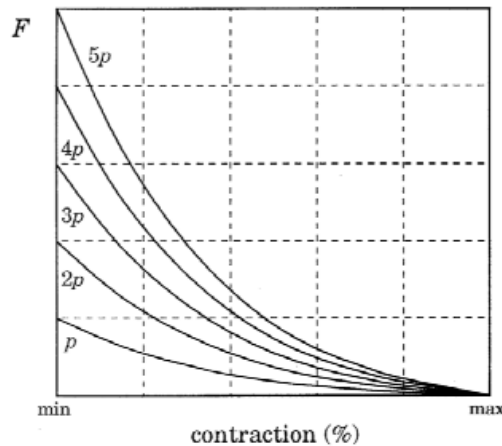


Figure 1.20: Daerden et al. (2002) found this force-contraction diagram for PAMs [11]. F = Force, p = pressure.

Non-linear behavior is more difficult to control compared to linear behavior of, for example, a cylinder-type pneumatic actuator. However, research on non-linear behavior of PAMs has been done, and control models are developed. A study by Tiziani et al. (2017) showed promising results for PAMs with position and force sensing capabilities, which allows prediction and control of the actuators [24].

To test the dissipation of forces, the muscles were tested at their maximum length (L_0) for 3 minutes at a pressure of $3bar$. The results showed that in three minutes forces would decrease with an average of $2.1 \pm 0.99N$. The outcome of the measured maximum output forces varied over different tests. The variation in forces can be explained by the fact that the actuators are made out of viscous material. The inner bladder of the actuator is composed of a balloon that stretches and could deform under high pressure, causing hysteresis. After a balloon has been under high pressure, it might not return back to its original state. When hysteresis occurs, energy dissipates due to internal friction of the material, and a lower output force is generated. The pneumatic actuator requires an initial length of $120mm$ to attain a stroke of $34mm$. Results show that the stroke of the muscles are

$20 - 24mm$, $22.5 - 27mm$, $25 - 30mm$, $27.5 - 33mm$, and $30 - 36mm$ for the muscles with an L_0 of $80mm$, $90mm$, $100mm$, $110mm$, and $120mm$ respectively. When a pneumatic muscle with an initial length of $120mm$ is taken into account, it can be seen that the pressure to reach $15N$ stays below $1.5bar$, which is lower than the maximum pressure a PAM can handle. This is a beneficial result since the stresses on the PAM will be lower. This will cause less internal friction and hysteresis of the balloon.

Stringpot

The distance sensor (stringpot) is developed to measure the position of the shoulder, which is the input for the prosthetic hand. An important aspect to change was the ability to continuously measure the distance while bending along the curvature of the shoulder. Besides that requirement, the system also had to be able to measure a change in distance of $34mm$.

The results show that the distance measured by the stringpot over three tests had a deviation between -1 and $1mm$ compared to the laser sensor. A study by Crago et al. (1986) regarding sensors in prosthesis design, stated that a resolution of a distance sensor should be at $1mm$, or $\frac{1}{3}$ degree, whichever value is smaller [25]. The largest deviation can be seen when the stringpot reaches its maximum value. Where the stringpot should reach $60mm$ according to our calculations, the practical reach was $58mm$, as seen in Figure 1.18, bottom plot. A practical reach of $58mm$ does not cause a problem, since the average maximum displacement of the shoulder is $34mm$. The size of the device can be improved, especially the height, to make it wearable underneath clothing. The dimensions could be reduced by evaluating different (smaller) key-retractors and/ or potentiometers. Also, the potentiometer is attached vertically, which increases the height noticeably. A design can be considered placing the potentiometer horizontally.

Recommendations

The developed prototype is small, lightweight, smooth-edged, and curves along the shoulder while still meeting the mechanical requirements. As compared to the systems of Vardy et al. (2017) and J. Lambers (2019), the developed system is substantially smaller, lighter in weight, has an overall more simple design, and curves along the shoulder. There is room for some improvement. The anchor system with the U-bolts should have a smoother top. The U-bolts with two nuts screwed on now sticks out. The

stringpot functions well up to a length of $58mm$, for future research it could be investigated whether this device can be made smaller in size. Also, no research was done on users, but solely on mechanical testing of the devices. It would be interesting to test this system on humans to test the applicability.

1.7. Conclusion

The goal of this study was to design and evaluate a pneumatic haptic interface device for an upper limb prosthesis, which was comfortable and aesthetically beautiful. The final design includes a pneumatic actuator (PAM) to provide feedback, an anchoring system to be placed on the scapula, and a distance sensor (stringpot) to measure the distance between the two anchor points. To reach high values of comfort and cosmetics, the design had to be small, lightweight, and smooth-edged. The results showed:

- The dimensions of the final design of the PAM and anchor system are $50 \times 25 \times 120mm$ and it weighs $41g$.
- Maximum output force of $104.8N$ is measured for a PAM with a L_0 of $120mm$.
- Maximum stroke of $30 - 36mm$ is measured for a PAM with a L_0 of $120mm$.
- An increasing pressure is required to reach an output force of $15N$ when the PAM contracts.
- The dimensions of the stringpot are $34mm$ in diameter and $41mm$ in height, and it weighs $29g$.
- The stringpot measures a difference in distance up to $58mm$ and has a deviation between $-1mm$ and $1mm$.

The results the design system showed, meet almost all pre-set requirements. The designed haptic system is small in size, lightweight, and smooth-edged, while still meeting the requirements regarding the mechanical properties of the system, which are promising results in terms of applicability in prosthesis design. Future research should be done involving human participants, to study the applicability of the device.

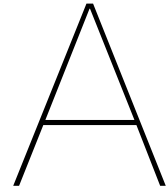
Bibliography

- [1] G Smit. Natural grasping, design and evaluation of a voluntary closing adaptive hand prosthesis. *TU Delft repository*, *repository.tudelft.nl*, 2013.
- [2] Kathryn Ziegler-Graham, Ellen J MacKenzie, Patti L Ephraim, Thomas G Trivison, and Ron Brookmeyer. Estimating the prevalence of limb loss in the united states: 2005 to 2050. *Archives of physical medicine and rehabilitation*, 89(3):422–429, 2008.
- [3] Gerwin Smit and Dick H Plettenburg. Efficiency of voluntary closing hand and hook prostheses. *Prosthetics and orthotics international*, 34(4):411–427, 2010.
- [4] Dick H Plettenburg. Prosthetic control: A case for extended physiological proprioception. In *University of New Brunswick's Myoelectric Controls/Powered Prosthetics Symposium*, pages 73–75, 2002.
- [5] Bartjan Maat, Gerwin Smit, Dick Plettenburg, and Paul Breedveld. Passive prosthetic hands and tools: A literature review. *Prosthetics and orthotics international*, 42(1):66–74, 2018.
- [6] Mona Hichert, Alistair N Vardy, and Dick Plettenburg. Fatigue-free operation of most body-powered prostheses not feasible for majority of users with trans-radial deficiency. *Prosthetics and orthotics international*, 42(1):84–92, 2018.
- [7] Alistair N Vardy, Manon Boone, and Dick H Plettenburg. Perceptual and control properties of a haptic upper-limb prosthetic interface. *Proceedings of MEC17*, 2017.
- [8] J.A.L. Lambers. Sensitivity and control of a pneumatic force transducer. *Delft University of Technology, 3me Biomedical Engineering*, pages 1–167, 2019.
- [9] Guido Belforte, Gabriella Eula, Alexandre Ivanov, and Silvia Sirolli. Soft pneumatic actuators for rehabilitation. In *Actuators*, volume 3, pages 84–106. Multidisciplinary Digital Publishing Institute, 2014.
- [10] Ioana Petre. Pneumatic muscle diameter evolution under compressed air action. *Journal of Electrical and Electronics Engineering*, 5(1):185, 2012.
- [11] Frank Daerden, Dirk Lefeber, et al. Pneumatic artificial muscles: actuators for robotics and automation. *European journal of mechanical and environmental engineering*, 47(1):11–21, 2002.
- [12] Dick H Plettenburg. Basic requirements for upper extremity prostheses: the wilmer approach. In *Proceedings of the 20th Annual International Conference of the IEEE Engineering in Medicine and Biology Society. Vol. 20 Biomedical Engineering Towards the Year 2000 and Beyond (Cat. No. 98CH36286)*, volume 5, pages 2276–2281. IEEE, 1998.
- [13] Dick H Plettenburg, Mona Hichert, and Gerwin Smit. Feedback in voluntary closing arm prostheses. In *Proceedings of the Myo Electric Control Symposium-MEC*, volume 11, pages 14–19, 2011.
- [14] Plettenburg Dick H Vardy, Alistair N. Control locations for harnesses used in upper limb prostheses. In *Delft University of Technology (DIP)*, pages 271 – 274, 2014.
- [15] M.M.B. Mastenbroek. Force-to-weight, power-to-weight, and energy-to-weight ratios of pneumatic actuators: an overview (msc literature study). *Delft University of Technology, 3me Biomedical Engineering*, pages 1–14, 2020.
- [16] Dick H Plettenburg. Pneumatic actuators: A comparison of energy-to-mass ratio's. In *9th International Conference on Rehabilitation Robotics, 2005. ICORR 2005.*, pages 545–549. IEEE, 2005.

- [17] Ching-Ping Chou and Blake Hannaford. Measurement and modeling of McKibben pneumatic artificial muscles. *IEEE Transactions on robotics and automation*, 12(1):90–102, 1996.
- [18] Shadow Robot Company. Shadow 30mm air muscle - specification S30AM-S-1. <https://www.shadowrobot.com/>, 2011. [Online; accessed 01-12-2020].
- [19] Mona Hichert and Dick H Plettenburg. Ipsilateral scapular cutaneous anchor system: An alternative for the harness in body-powered upper-limb prostheses. *Prosthetics and Orthotics International*, 42(1):101–106, 2018.
- [20] FUTEK advanced sensor technology. FUTEK load cell LSB200. <https://www.futek.com/store/load-cells/s-beam-load-cells/miniature-s-beam-LSB200>, 2021. [Online; accessed 17-03-2021].
- [21] SCAIME. SCAIME CPJ - CPJ2S analog signal conditioner. <https://scaime.com/product/post/cpj---cpj2s>, 2021. [Online; accessed 17-03-2021].
- [22] National Instruments. NI USB 6211 multifunctional device. <https://www.ni.com/nl-nl/support/model.usb-6211.html>, 2021. [Online; accessed 17-03-2021].
- [23] T. Nagarajan, S. Lirishnan, V. Amirtham, A. M. Abdul-Raniand, and T. V. V. L. N. Rao. Experimental investigation-natural fiber braided sleeve for pneumatic artificial muscles actuation. *Asian Journal of Scientific Research*, 6(3):596–602, 2013.
- [24] Lucas O Tiziani, Thomas W Cahoon, and Frank L Hammond. Sensorized pneumatic muscle for force and stiffness control. In *2017 IEEE International Conference on Robotics and Automation (ICRA)*, pages 5545–5552. IEEE, 2017.
- [25] Patrick E Crago, Howard J Chizeck, Michael R Neuman, and F Terry Hambrecht. Sensors for use with functional neuromuscular stimulation. *IEEE Transactions on Biomedical Engineering*, (2):256–268, 1986.
- [26] Ecaterina Vasluian, Corry K van der Sluis, Anthonie J van Essen, Jorieke EH Bergman, Pieter U Dijkstra, Heleen A Reinders-Messelink, and Hermien EK de Walle. Birth prevalence for congenital limb defects in the northern netherlands: a 30-year population-based study. *BMC musculoskeletal disorders*, 14(1):323, 2013.
- [27] C.K. Van der Sluis and M.A.H. Brouwers. Een armamputatie of een transversaal congenitaal reductiedefect. in: *Revalidatie voor volwassenen*. pages 177–245, 2014.
- [28] Maurice A LeBlanc. Innovation and improvement of body-powered arm prostheses: A first step. *Clin Prosthet Orthot*, 9(1):13–16, 1985.
- [29] Elaine Biddiss and Tom Chau. Upper-limb prosthetics: critical factors in device abandonment. *American journal of physical medicine & rehabilitation*, 86(12):977–987, 2007.
- [30] Debra Ann Latour. Method for anchoring prosthetic and orthotic devices, September 2 2014. US Patent 8,821,588.
- [31] Mona Hichert, David A Abbink, Alistair N Vardy, Corry K van der Sluis, Wim GM Janssen, Michael AH Brouwers, and Dick H Plettenburg. Perception and control of low cable operation forces in voluntary closing body-powered upper-limb prostheses. *PloS one*, 14(11):e0225263, 2019.
- [32] D Latour, T Sabolevski, and K Lajoie-Weaver. Ipsilateral scapular cutaneous anchor. In *Proceedings of the 12th world congress of the International Society for Prosthetics and Orthotics*, 2007.

- [33] Kristin Østlie, Ingrid Marie Lesjø, Rosemary Joy Franklin, Beate Garfelt, Ola Hunsbeth Skjeldal, and Per Magnus. Prosthesis use in adult acquired major upper-limb amputees: patterns of wear, prosthetic skills and the actual use of prostheses in activities of daily life. *Disability and Rehabilitation: Assistive Technology*, 7(6):479–493, 2012.
- [34] Antony Barber. *Pneumatic handbook*. Elsevier, 1997.
- [35] Hazem I Ali, SBBM Noor, SM Bashi, and MH Marhaban. A review of pneumatic actuators (modeling and control). *Australian Journal of Basic and Applied Sciences*, 3(2):440–454, 2009.
- [36] G. Granosik and J. Borenstein. Minimizing air consumption of pneumatic actuators in mobile robots. In *Proceedings - IEEE International Conference on Robotics and Automation*, volume 2004, pages 3634–3639, 2004.
- [37] Festo. Fluidic muscle dmps/ mas. *Festo Brouchure Fluidic muscle*, 2004.
- [38] Leonardo Cappello, Kevin C Galloway, Siddharth Sanan, Diana A Wagner, Rachael Granberry, Sven Engelhardt, Florian L Haufe, Jeffrey D Peisner, and Conor J Walsh. Exploiting textile mechanical anisotropy for fabric-based pneumatic actuators. *Soft robotics*, 5(5):662–674, 2018.
- [39] H.F. Schulte. The characteristics of the mckibben artificial muscle. the application of external power in prosthetics and orthotics. *Washington, D. C., National Academy of Sciences—National Research Council. Publication 874*, page 94–115, 1961.
- [40] DG Caldwell, GA Medrano-Cerda, and MJ Goodwin. Braided pneumatic actuator control of a multi-jointed manipulator. In *Proceedings of IEEE Systems Man and Cybernetics Conference-SMC*, volume 1, pages 423–428. IEEE, 1993.
- [41] Darwin G Caldwell, N Tsagarakis, D Badihi, and Gustavo A Medrano-Cerda. Pneumatic muscle actuator technology: a light weight power system for a humanoid robot. In *Proceedings. 1998 IEEE International Conference on Robotics and Automation (Cat. No. 98CH36146)*, volume 4, pages 3053–3058. IEEE, 1998.
- [42] Blake Hannaford, Jack M Winters, Ching-Ping Chou, and Pierre-Henry Marbot. The anthroform biorobotic arm: a system for the study of spinal circuits. *Annals of biomedical engineering*, 23(4):399–408, 1995.
- [43] K. C. Wickramatunge and T. Leephakpreeda. Study on mechanical behaviors of pneumatic artificial muscle. *International Journal of Engineering Science*, 48(2):188–198, 2010.
- [44] Vishay. Potentiometer Vishay from Conrad. <https://www.conrad.nl/p/vishay-249fgjs0xb25103ka-precisiepotmeter-mono-1-w-10-k-1-stuks-424170>, 2021. [Online; accessed 17-04-2021].

Appendices



Background

The objective of the background analysis is to gain insight into the existing prostheses, harnesses, the available actuators, and the state of the art.

A.1. Upper limb deficiency

Upper limb deficiency is a condition where a part of the upper limb is missing. This condition can be caused by a congenital defect or an acquired defect due to trauma. In a congenital defect, a baby is born with an underdeveloped upper extremity. This could be due to a genetic defect or an environmental cause. With an acquired defect due to trauma, the patient suddenly loses (part of) an arm and has to adjust their way of living. A person born with an underdeveloped upper extremity doesn't know any different and is used to executing tasks with their stump or prosthesis since they were born. On the other hand, when the deficiency is caused by trauma, the person has to adjust their life dramatically and find solutions for all their activities of daily living (ADL's).

Overall, the prevalence of this condition is low. In The Netherlands the prevalence of congenital defects was around 2.9 per 10.000 births [26]. Besides that, about 50 people per year lose an arm or a hand (wrist articulation level or more proximal), of which 70% is due to trauma. The rest is caused by oncological processes, infectious diseases, vascular problems or chronic pain [27]. Other studies show a prevalence of 0.8 per 10.000 inhabitants in The Netherlands and 1.4 per 10.000 in the United States of America [1, 2].

A.2. Upper limb prostheses

Arm prostheses are important for upper limb amputees to ensure optimal functional rehabilitation. There are different kinds of upper limb prostheses, which can be divided into two categories; passive and active prostheses. Passive prostheses are actuated by an external power source, for example, the other hand. Active prostheses are actuated internally by, for example, an electric, a hydraulic, or a pneumatic actuator.

A.2.1. Passive prostheses

Passive prostheses include prosthetic hands and prosthetic tools. Prosthetic hands replace the missing hand with a fabricated, real-looking one. Prosthetic tools are mainly meant to enable specific tasks (such as sports, chores, driving a car) and have a more mechanical look. Prosthetic hands are meant to give an aesthetic replacement. Examples can be seen in Figure A.1.

A.2.2. Active Prostheses

Active prostheses can be divided into body-powered (BP) and externally powered prostheses. A body-powered prosthesis is often actuated by pulling a Bowden cable which causes the terminal device to open or close. The terminal device (TD) can be a hook or a hand. The Bowden cable is often pulled by generating forces using a harness and making gross body movements. The BP prosthesis can be voluntary opening (VO) or voluntary closing (VC). In a prosthesis with a terminal

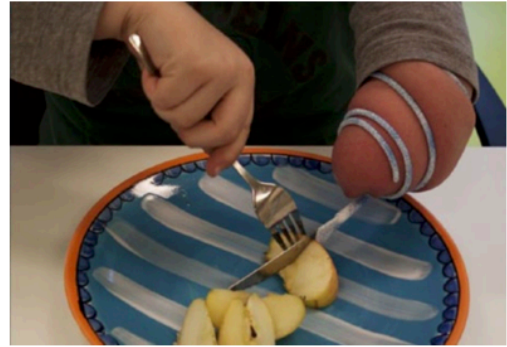


Figure A.1: Prosthetic hand (l) and prosthetic tool (r). Adjusted from [5].

device that includes VO, the user has to apply a force to the cable to close the TD, where-after a spring mechanism returns the hand to the opened position. Whereas with a VC prosthesis, the mechanism works in the opposite direction and opens when a force is applied to the Bowden cable. Figure A.2 shows the mechanism of such a BP prosthesis with Bowden cable that is pulled by generating shoulder movements. Body-powered prostheses can be controlled by other movements than shoulder movements, such as the elbow-controlled WILMER prosthesis [12].

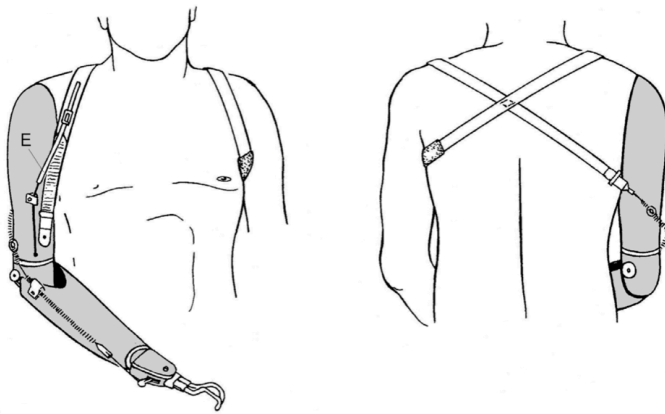


Figure A.2: Body-powered prosthesis, including the harness and Bowden cable.

A.2.3. Externally powered prostheses

Externally powered prostheses have an external power source, such as an electric, hydraulic or pneumatic actuator. Usually, electromyography signals (EMG) control the terminal device of these prostheses. Unaffected muscles generate EMG signals when they contract. These signals can be recorded by EMG electrodes, which can be stuck to the skin. When the muscle is contracted, the fire rate of the muscle increases, which is read by the system, and this will then result in an action of the TD of the prosthesis. In this way, the patient can control the opening and closing of the TD.

A.3. Harness system

A.3.1. Harness control by shoulder movements

Body-powered prostheses use a shoulder harness and steel cables (Bowden cables) to control the terminal device [28]. The movements of the shoulder to control the prosthesis include elevation/depression and retraction/protraction. Elevation is the upwards movement of the shoulder joint, depression includes the downwards movement. Retraction of the shoulder involves moving the scapula's towards each other, whereas protraction is the opposite movement and the scapula's move away from each other, see Figure A.3.

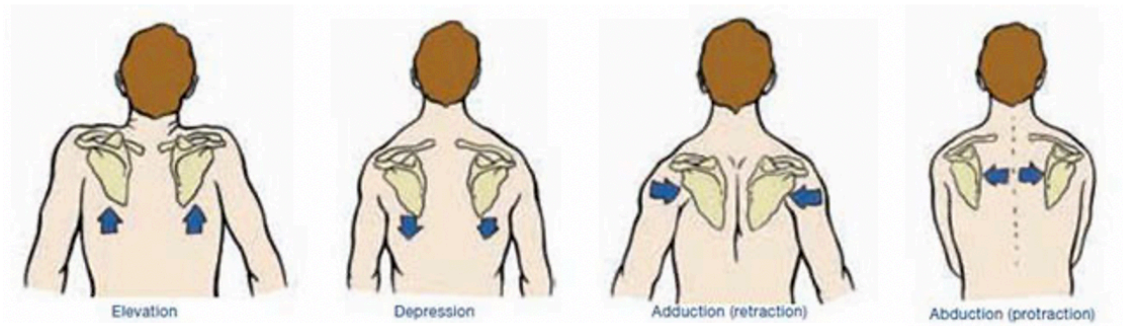


Figure A.3: The shoulder movements (fltr): elevation, depression, retraction, protraction

The prosthesis is controlled by a harness and the Bowden cable; the shoulder movements cause the Bowden cable to be pulled. The forces needed to pull the Bowden cable and operate the terminal device of the prosthesis are quite high. Powerful body movements are needed to reach these high control forces. Protraction and retraction of the shoulder are powerful body movements and thus very suitable to control an upper extremity prosthesis. Another advantage of the shoulder as a controlling body part is that shoulder movements of the contralateral side do not affect the orientation of the prosthesis and its terminal device. Research has been done to lower these control forces. However, attempts have failed and the harness design has not changed much over the past years [7].

A.3.2. Traditional harness design

The commonly used harness is the figure-of-8 or figure-of-9 harness, see Figure A.4. The harness consists of a loop around the contralateral shoulder, and a Bowden cable runs down to the prosthesis to control opening and closing. By moving the shoulder – elevation/depression and retraction/protraction – the cable to the terminal device is pulled, causing the opening or closing of the device. This harness is considered quite uncomfortable. It fits tightly around the user and causes pain in the neck, armpit, and upper back by rubbing of the harness on the skin. Besides this, patients do not like the aesthetics of the harness, since this is visible through clothing. Sometimes clothing gets damaged by the harness. Of prosthesis users that rejected their prosthesis and stopped using it, 74% stated that they would consider using it again if technological improvements were done. They are significantly less satisfied with all aspects of comfort, ease of use, ease of control, reliability, and costs [29].

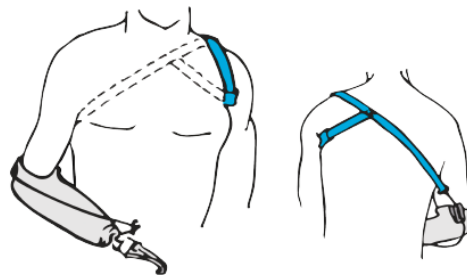


Figure A.4: A regular shoulder harness.

A.3.3. Alternative harness design

Debra Latour found an alternative for the harness system, called the Ipsilateral Scapular Cutaneous Anchor System [30]. This system does not have the straps of a harness, but attaches the Bowden cable directly to the skin with a so-called 'skin anchor'. This skin anchor is a plastic sticker that adheres to the users' skin with adhesive tape. The sticker is placed on the ipsilateral side, on the

scapula. Removing the straps of the regular 'figure of 8' or 'figure of 9' harness reduces the discomfort since there is no more rubbing of the straps in the neck or armpit [19, 31, 32].

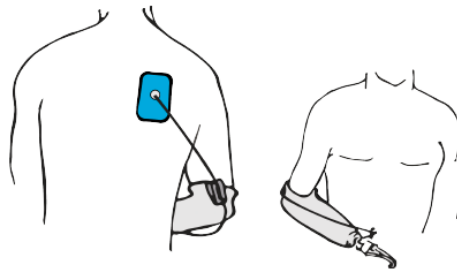


Figure A.5: The anchoring system of Debra Latour [32].

A.4. Cosmetics, comfort and control

Although most amputees receive a prosthesis after the loss of (part of) the upper extremity, the percentage of long-term wearers varies substantially [4, 33]. Twenty to forty percent of patients with an amputation of their upper extremity do not wear and use a prosthesis. Besides that, around 50% of the people wearing their prosthesis, do this for aesthetic reasons [4]. Many patients decide not to wear the prosthesis because they are heavy, uncomfortable, unnecessary, or they don't like the appearance. Also, they find that many activities of daily living (ADL's) can be executed single-handedly. Development of prostheses should thus focus on cosmetics, comfort and control (the three C's) [4, 5, 12]. Each of the different types of prostheses has its advantages and disadvantages regarding cosmetics, comfort, and control.

The cosmetic value of a prosthesis implies the subjective opinion of the aesthetics regarding their prosthesis [12]. It is often considered aesthetically beautiful when the prosthesis resembles a real hand. Besides this, it should be small, lightweight, non-contaminating, and smooth-edged.

The fitting and the weight of the prosthesis largely affect the comfortability. The transmission of forces from the patient to the prosthesis should be as smooth as possible with low friction forces. Forces perpendicular to the skin are mostly opposed by the skin, but as soon as the forces direct in the plane of the skin, shear forces arise which causes damage to the skin. High operating forces cause fatigue and discomfort with the user. Research done by Hichert, Vardy, and Plettenburg (2018) showed that operation forces should be maximum $38N$ for females and $66N$ for males to achieve fatigue-free operation of body-powered prostheses [6]. Besides low operating forces, the weight is also important; A heavy prosthesis is often considered as uncomfortable. Patients also prefer a device that has a good fitting and can be donned on and off easily [12].

The quality of the control of the prosthesis contributes to how easily the device can be used. Systems that include feedback are in all cases easier to control than without. Regarding the control of upper extremity prostheses, proprioceptive feedback is an important source of information. Proprioceptive feedback is the subconscious knowledge of self-movement and body position. The muscle length, velocity of contraction, and force the muscle exerts are sensed by muscle spindles and Golgi tendon organs (GTO), positioned within the muscles and tendons. The information of the muscle spindles and GTOs is fed back to the central nervous system (CNS). With body-powered prostheses, the GTOs sense the magnitude of the muscle force pulling the Bowden cable. Besides this, the harness and socket of BP prostheses give pressure and friction to the skin. The skin sends these signals to the CNS, providing more information about the magnitude of the force used on the BP prosthesis.

A.4.1. Advantages and disadvantages

Prosthetic hands and tools

Of all upper extremity prostheses, prosthetic hands look the most like regular hands. Besides this, they are very simple, lightweight, and relatively cheap. However, they are static and the hand or other terminal device does not move. Therefore, they might be less functional than body-powered or externally powered prostheses.

Body-powered prostheses

Advantages of body-powered prostheses are their simplicity, their light weight, and the established proprioceptive feedback.

The feedback of the force with which the patient is pulling the cable - and thus closing or opening the TD - provides valuable information. The presence of feedback is important in upper extremity prostheses as it improves the control of the prosthesis and improves the execution of daily tasks that require fine motor adjustments [7]. An advantage of a VO prosthesis is that once the object is grasped, no more force is needed to maintain the grasping position, the spring inside the system does this for you. A disadvantage of this is that the grasping force depends completely on the type of spring that is built inside the system and can not be controlled by the patient him/herself. The VC prosthesis has the advantage that the grasping force is independent of the spring inside the system, and thus a larger grasping force can be generated. The disadvantage of this is that it can be tiring to hold an object for a longer period of time. An overall disadvantage of BP prostheses is the harness needed to wear them. This is often considered uncomfortable and annoying. Also, the physical effort it requires to control the prosthesis is rather high, making it even more uncomfortable to use.

Externally powered prostheses

Since the output power of externally powered prostheses does not depend on forces generated by the patient itself, the output force can be higher compared to BP prostheses. On one hand, it is a big advantage that the patient does not need to provide these forces since this can be quite tiring. On the other hand, the absence of the Bowden cable results in a large disadvantage; there is only visual feedback and no proprioceptive feedback. This results in a more challenging control of the prostheses, and thus often a longer training period is necessary to comfortably use this type of prosthesis. In general, externally powered prostheses are relatively heavy weight which could make them uncomfortable to wear. Besides this, they are often expensive and require a lot of maintenance.

A.5. New designs including feedback

To combine the advantage of both a body-powered prosthesis (feedback) and an externally powered prosthesis (low operation forces), a new prosthesis design was proposed. A study by Vardy et al. (2017) at the *Delft Institute of Prosthetics and Orthotics* (DIPO) proposed a design focused on the main advantage of a BP prosthesis (the proprioceptive force feedback) but at the same time eliminates the harness and its additional discomfort and high operation forces. The design includes a haptic interface that provides proprioceptive force feedback while allowing the user to control the prosthesis within a comfortable force range. It consists of a master system, controlled by the shoulder and a slave system, which is the externally powered hand prosthesis. The master system is attached to the shoulder by skin anchors and controlled by movements of the shoulder. These movements are the same as those controlling BP prostheses. The proprioceptive force feedback is provided by pulling the skin anchors closer together. The main advantage of using skin anchors would be that they fit easily underneath clothing, improving cosmetics [7]. Besides this, the control and comfort will be improved as well, so the demands of prosthetic design (the three C's) will be met. The conceptual design can be seen in Figure A.6. The design of this device is not yet entirely elaborated. One aspect that needs to be improved and clarified is the actuator placed between the skin anchors. This study of Vardy et al. (2017) included an electrical actuator, but was not wearable at all. Another study included a pneumatic actuator to actuate the skin anchors and showed promising results. The design was wearable, but still quite large, heavy, and bulky [8].

A.6. Actuators

Proprioceptive force feedback needs to be provided through these anchor points on the scapula. This will be done by pulling the two anchor points towards each other, as a counteracting force. It is important to choose a suitable actuator to exert these forces. There are numerous kinds of actuators; hydraulic, electric, pneumatic, and thermal actuators.

Hydraulic actuators are driven by fluids. They consist of a piston with two chambers. Adding liquid to one chamber causes a piston rod to move, resulting in an exerting force. Electric actuators are driven by a linear or rotary motor. Pneumatic actuators are driven by compressed air, which they convert into linear or rotary movements [34].

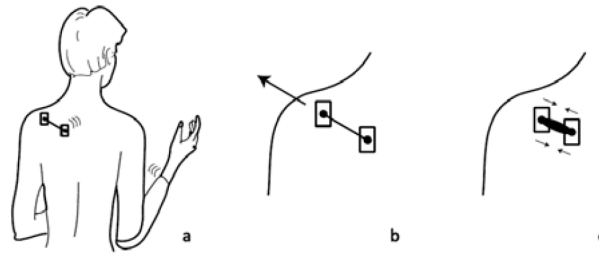


Figure A.6: The proposed design of the haptic interface by Vardy et al. (2017). (a) the skin anchors with wireless connection to the prosthetic hand, (b) movements of the shoulder control the device, (c) proprioceptive feedback is provided by pulling the skin anchors closer together. The figure is retrieved from [7].

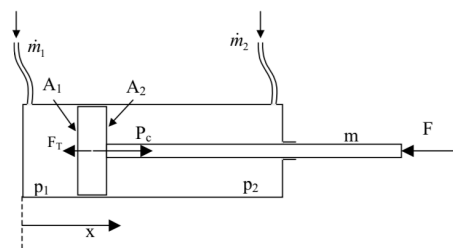
Hydraulic actuators are subjected to temperature limitations and need fluid return lines [35]. They are not considered useful in prosthesis design with the actuator placed close to the skin of a user.

Pneumatic actuators are lightweight, safe, compact, agile, easy to install and they require overall low maintenance [9–11]. They are considered suitable in prosthesis design. On the other hand, electric actuators are more accurate compared to pneumatic actuators. The study of J. Lambers [8] showed that the accuracy of pneumatic actuators is high enough for this type of design.

Within pneumatic actuators a distinction can be made between piston in cylinder actuators, rotary vane actuators, soft pneumatic actuators, and artificial muscles.

A.6.1. Piston in cylinder actuators

Piston-in-cylinder actuators, or pneumatic cylinders, consist of two chambers and a piston rod. Changing the pressure in one of the chambers by inlet or outlet of compressed air causes the piston rod to move, resulting in an output force. A distinction is made between single-acting and double-acting cylinders. A single-acting cylinder can only exert force in one direction and returns to the starting position without supply of compressed air. It can contain, for example, an internal spring that pushes the piston rod back to its original position. A double-acting cylinder can exert a force in two directions. The direction of the force depends on in which room the compressed air is added, or removed. A schematic drawing of a pneumatic cylinder can be seen in the figure below. This is a double-acting cylinder. Adding air to m_1 results in the piston rod moving to the right regarding the x-axis. Whereas addition of air to m_2 would result in moving the rod to the left [36].



(a) Schematic drawing of a pneumatic cylinder. Retrieved from [36].



(b) Pneumatic cylinder from FESTO bv. Retrieved from [37].

Figure A.7: Pneumatic cylinder; schematic drawing and an example of a cylinder of FESTO.

A.6.2. Rotary vane actuators

Rotary vane actuators, or just rotary actuators, convert the energy of compressed air into rotational movement. It consists of a rotor with vanes attached to it, placed in a chamber. When compressed air is let into the chamber the vanes turn, resulting in the rotary movement.

A.6.3. Soft pneumatic actuators

Soft pneumatic actuators is an umbrella term for actuators designed to be flexible and soft, for example, textile actuators. These actuators are made of a fabric in which small chambers are

processed, to let compressed air in. Many of these actuators rely on elastomeric materials [15, 38].

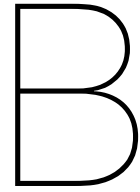
A.6.4. Pneumatic Artificial Muscles

In 1950, the first pneumatic artificial muscle (PAM) was engineered by Joseph L. McKibben and was designed to be used in an upper-extremity prosthesis. A PAM is also referred to as a McKibben muscle. This pneumatic actuator is commonly used in prostheses [39–42]. A PAM consists of a flexible bladder inside an outer braided mesh. When the bladder inflates, it will extend against the outer mesh. The initial length (L_0) is the length of the muscle when the pressure is equal to the pressure of the surrounding. L_{min} is the length of the muscle at maximum contraction. The diameter of the muscle will increase, while the length of the muscle decreases, keeping the volume nearly equal. This shortening of the actuator results in a pulling force that is generated [43].

The way PAMs function is by contracting by increasing the diameter. The inner balloon blows up, pushing to the outer shell and increasing in diameter. The outer shell causes the muscle to shorten. When the pressure within a PAM increases and the load does not change, then the muscle will contract. And when the pressure stays equal, but the load decreases, the muscle will contract as well. A PAM can only contract up to a certain point. When that happens, and the minimum length is reached, the output force also reaches a minimum [11, 23]. An example of a PAM can be seen in Figure A.8



Figure A.8: A pneumatic artificial muscle. Retrieved from [18].



Final design

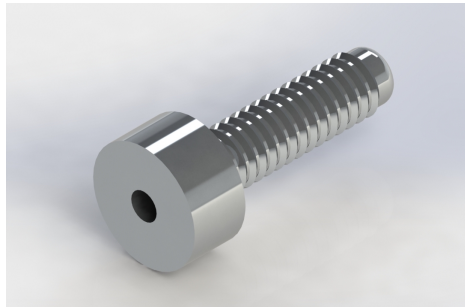
A detailed description of the design of the haptic system is provided here. The design of the system was divided into three parts: the pneumatic actuator, the anchor system, and the distance sensor. The choice of materials is elaborated, how the parts were produced is explained, and 3D-renders are presented.

B.1. Pneumatic artificial muscle

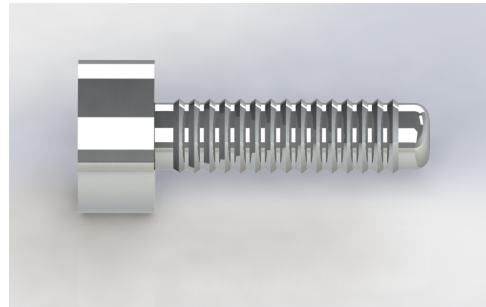
For this design, a pneumatic artificial muscle was considered to be the most suitable actuator. A PAM can be produced out of soft materials so it can bend along the curvature of the shoulder. As it must be worn under clothing, soft materials will be more fitting than a pneumatic cylinder. For the design of the PAM many materials for the inner balloon were considered. The material had to be strong enough to resist a pressure of around 3bar , and have a thin wall thickness so it would expand in diameter, but not break or tear. Multiple silicon tubes were tested, with a varying wall thickness. Tubes with a diameter of $6 - 9\text{mm}$ (so 6mm inner diameter, 9mm outer diameter), $6 - 10\text{mm}$ and $4 - 6\text{mm}$ were tested, but neither of them was suitable. When a pressure of more than 3bar was put on the tubes, they did not expand at all. Then, a company from The Netherlands, called Palmedic, offered to fabricate some tubes made from polyurethane. They fabricated tubes with a diameter of 4mm , 6mm , 8mm , and 10mm all with a wall thickness of 0.5mm . These tubes broke above a pressure of 1bar . First, they stretched and did not return to their original shape. When put under large pressure, they all burst. Finally, modeling balloons were tested. These balloons were strong enough to handle a pressure up to 3.5bar . They stretched and returned to their original shape. A cable sleeve was used as an outer mesh and worked perfectly. Because of the angle in which the material is woven, it shortens when the balloon enlarges in diameter. The balloon and the outer mesh needed to be attached to an end part that closes the balloon and mesh off. One end part also needed to include an m3 screw thread to attach the compressed air to. The parts were drawn in SolidWorks, see Figure B.1 .

The ridges of the end parts were added to create friction and obstruct the balloon and outer mesh from sliding off easily. One part includes a M3 screw thread and is hollow to let the compressed air in. The other part is closed off. The diameter of the end parts was chosen in such a way that the balloon would fit easily, and perfectly around the end parts. To minimize air leakage, shrink tubing was put around the balloon's endings.

To keep everything clamped onto the end parts and prohibit the balloon and outer mesh from sliding off when the pressure is increased, strong clamps were necessary. In the beginning, hose clips and tie wraps were considered. Hose clips did not fit perfectly which resulted in air leaking. Tie wraps did not clamp enough, they were very difficult to fasten tight enough. The tie wraps could not handle the high pressure and slid off easily. In the end, U-bolts were tested, and together with the stickers of the anchor system everything closed well enough and it could be tightened well.



(a) End part, with an m3 screw thread and is hollow to allow air to pass through.



(b) End part, side view. This part is not hollow, to close off the balloon.

Figure B.1: 3D-renders of the end parts of the PAMs.

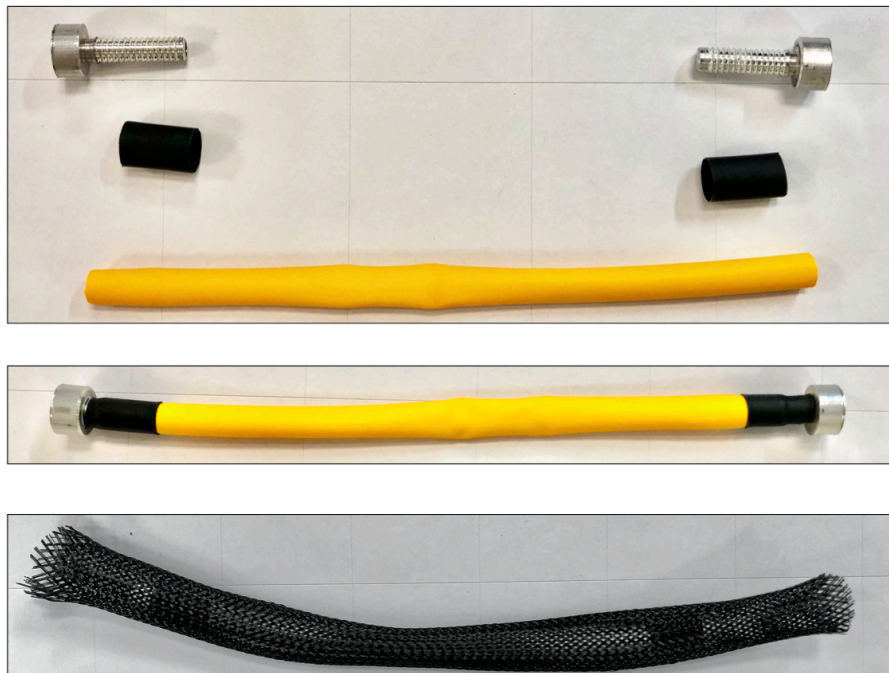


Figure B.2: Assembly of a PAM. Upper image: 2 end parts, (black) heat shrink, and a (yellow) balloon. Middle image: the balloon is attached to the end parts, and heat shrink is added to close it off. Bottom image: the cable sleeve is put around the balloon.

B.2. Anchor system

The anchor system was made to ensure the muscle with its end parts, the balloon, outer mesh and U-bolts would fit in perfectly. And besides that would be comfortable to wear and applicable to the skin of the shoulder of the user. Since 3D-printing allows a high level of customization and is quick, cheap and easy, this method was chosen. In addition, it is possible to print with materials that are flexible when printed very thin. MP Flex material from Makerpoint is such a flexible material. This material has a diameter of $2.85mm$ and was printed with the following printer settings:

Default printing temperature	$200^{\circ}C$
Default build plate temperature	$100^{\circ}C$
Retraction distance	$4.50mm$
Standby temperature	$175^{\circ}C$
Fan speed	100%
Layer height	$0.15mm$
Infill	20%

Table B.1: Printer settings of Ultimaker S3.

The design includes a hole in the frontal side to fit the PAM through, two holes in the top for the U-bolt to pass through, and a hole in the bottom where the u-bolt enters around the actuator. The bottom flat part of the sticker is printed $0.5mm$ thick, which leaves it flexible since it was printed with flexible print material. Figure B.3 shows the 3D-renders of the sticker. An assembly of both the actuator and the stickers is shown below, including an overview, top view and bottom view (Figures B.4 B.5, and B.6). And finally, a photo of an assembled PAM and anchor system is shown in Figure B.7.

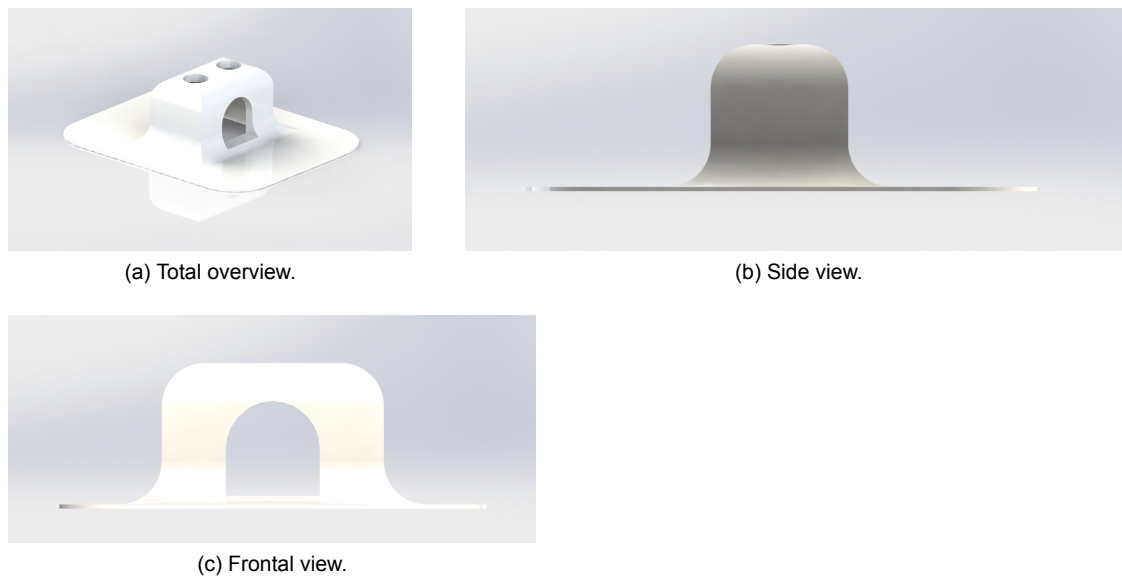


Figure B.3: 3D-renders of the skin anchors.

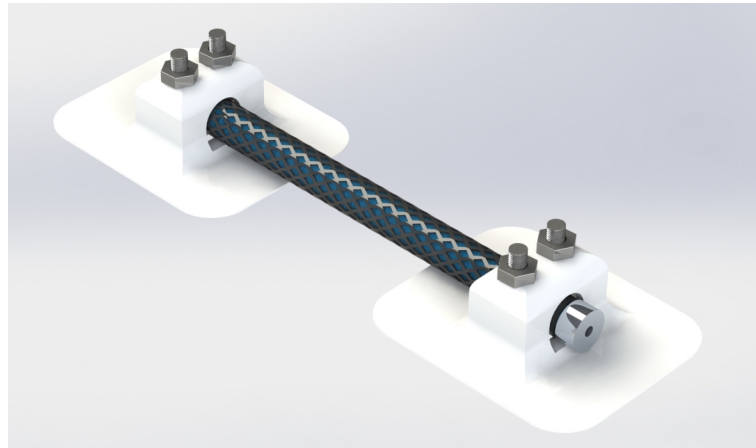


Figure B.4: 3D-render of a total overview of the overall system.

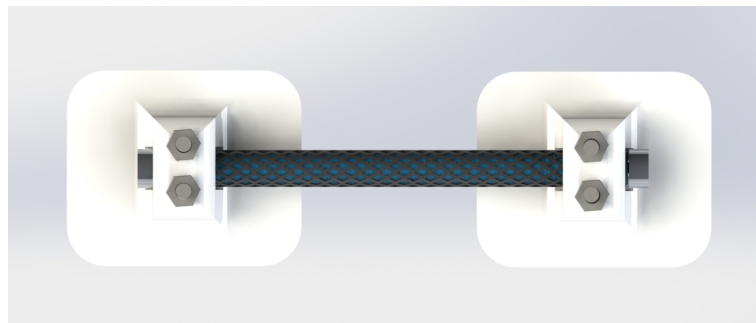


Figure B.5: 3D-render of the top view of the overall system.

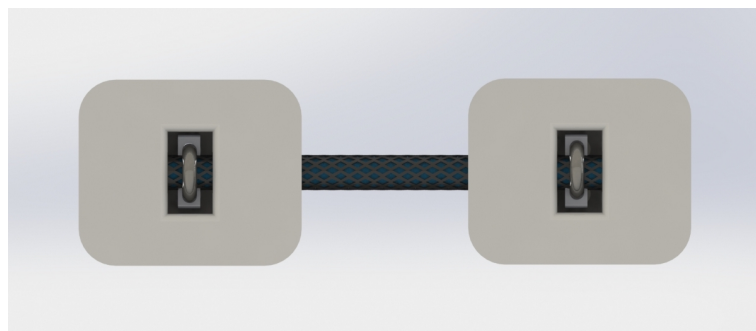


Figure B.6: 3D-render of the bottom view of the overall system.



Figure B.7: An assembled PAM with anchor system.

B.3. Stringpot

To measure the distance a string potentiometer, or stringpot, was designed. The system consists of a key-retractor that turns when the cable is pulled. A rotary potentiometer is attached to the key-retractor with a 3D-printed attachment piece. Thus, when the key-retractor turns it also turns the potentiometer. The signal of the potentiometer can then be used to calculate the distance since it is known how much distance the cable travels during one turn.

The box has a diameter to exactly fit the key-retractor in it. The lid of the box has a hole that exactly fits the bolt of the potentiometer so it would be secured onto the box to allow only the bottom part of the potentiometer to turn. The attachment piece has five prongs with the same diameter as the turning part of the key retractor. When the key-retractor turns, the attachment piece turns. The turning part of the potentiometer fits exactly into the tube-part of the attachment piece to ensure that the potentiometer turns when the key-retractor and attachment piece turn. The box, lid, and attachment piece were printed using tough black PLA, and PVA as support material with the following printer settings:

Default printing temperature	225°C
Default build plate temperature	60°C
Retraction distance	6.50mm
Standby temperature	175°C
Fan speed	100%
Layer height	0.15mm
Infill	20%

Table B.2: Printer settings of Ultimaker S3.

The figures below show 3D-renders of the designed box, lid and attachment piece. Also, an assembly and cross-section of the stringpot are shown in Figure B.11. Figure B.12 shows the printed parts and the assembled system. The potentiometer used is a single turn, linear, rotary potentiometer of Vishay [44]. And an Arduino UNO was used to read the output signal and send it to a laptop. Figure B.13 shows the connection of the potentiometer to the Arduino.

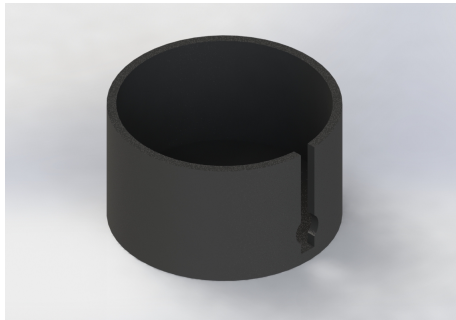
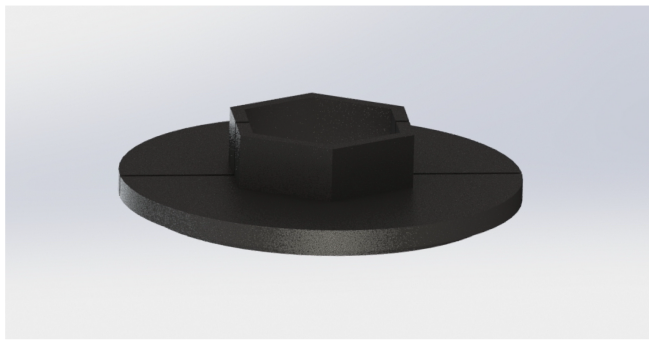
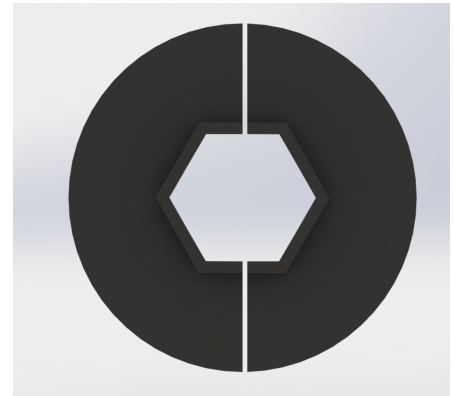


Figure B.8: 3D-render of the designed box.



(a) Total overview.



(b) Top view.

Figure B.9: 3D-renders of the designed lit.



(a) Total overview.



(b) Top view.

Figure B.10: 3D-renders of the designed attachment piece.

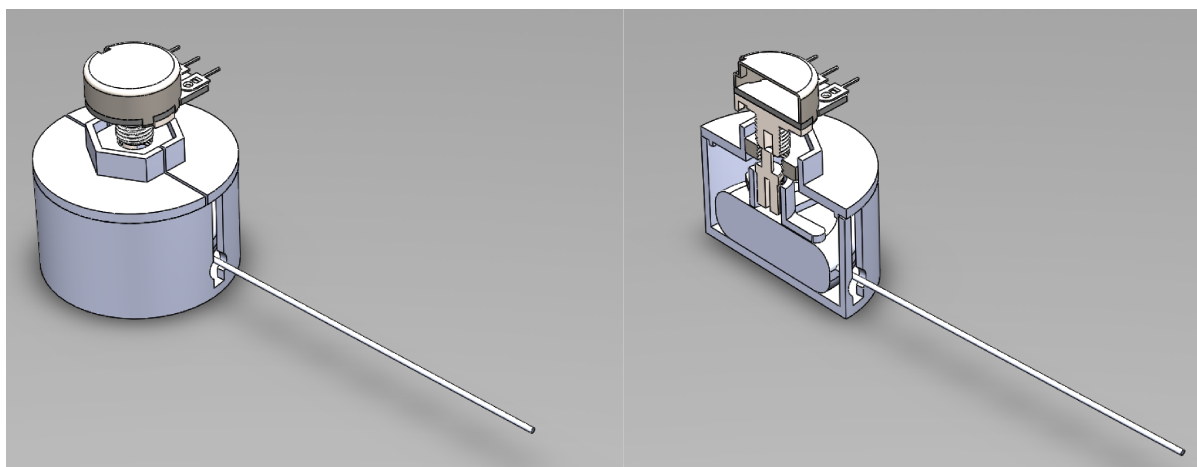


Figure B.11: 3D-renders of the assembled stringpot and its cross-section.



Figure B.12: The stringpot printed parts and the assembled stringpot.

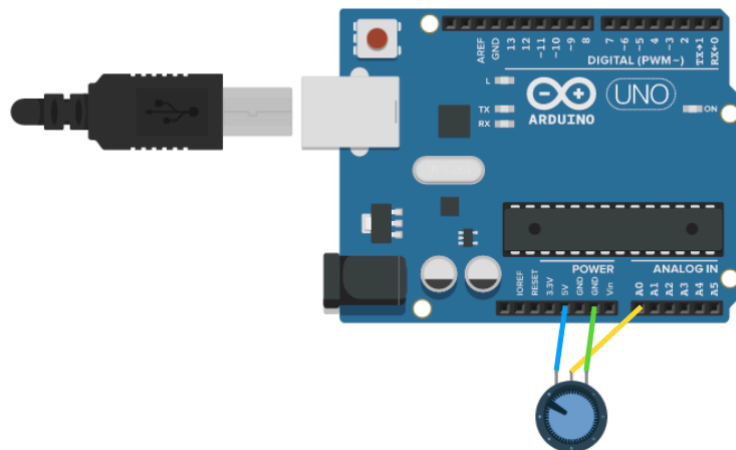
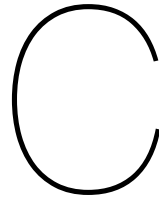


Figure B.13: Connection scheme of the potentiometer to the Arduino. The blue wire is connected to 5V, the green wire to GND (ground), and the yellow wire to an analogue input A0.



MATLAB code

C.1. Script mechanical tests muscles Force

```
1 clear all;
2 close all;
3 clc;
4
5 % Script thesis Merel Mastenbroek
6 % 06-04-2021
7 % Calculating force-length and force-contraction relationship
  of PAMs
8
9 %% L0 = 80mm
10 % loading data
11 data_m7t3 = load('/Users/merelmastenbroek/Allemaal Bestanden/
  BME/Afstuderen/Data-files/Data/21 02 23 14 25 34 muscle7-
  test3.txt');
12
13 % define L0 of the muscle
14 l0_m7t3 = 80;
15
16 %calculate length, contraction, forces using function '
  loopdata'
17 [xaxis_m7t3, mean_F_m7t3, lmin_lmax_gemF_m7t3, L_op_Fmax,
  Fmax, contraction_m7t3] = loopdata(data_m7t3, l0_m7t3);
18
19 data_m7t2 = load('/Users/merelmastenbroek/Allemaal Bestanden/
  BME/Afstuderen/Data-files/Data/21 02 23 14 21 30 muscle7-
  test2.txt');
20 l0_m7t2 = 80;
21 [xaxis_m7t2, mean_F_m7t2, lmin_lmax_gemF_m7t2, L_op_Fmax,
  Fmax, contraction_m7t2] = loopdata(data_m7t2, l0_m7t2);
22
```



```

23 data_m7t1 = load(' /Users/merelmastenbroek/Allemaal Bestanden/
    BME/Afstuderen/Data-files/Data/21 02 23 14 15 00 muscle7-
    test1.txt ');
24 l0_m7t1 = 80;
25 [xaxis_m7t1, mean_F_m7t1, lmin_lmax_gemF_m7t1, L_op_Fmax,
    Fmax, contraction_m7t1] = loopdata(data_m7t1, l0_m7t1);
26
27 Gem_F_m7 = ((mean_F_m7t1 + mean_F_m7t2 + mean_F_m7t3)./3);
28 Fmax_80 = Fmax
29 %% L0 = 90 mm
30 data_m6t1 = load(' /Users/merelmastenbroek/Allemaal Bestanden/
    BME/Afstuderen/Data-files/Data/21 02 19 13 35 52 muscle6-
    test1.txt ');
31 l0_m6t1 = 90;
32 [xaxis_m6t1, mean_F_m6t1, lmin_lmax_gemF_m6t1, L_op_Fmax,
    Fmax, contraction_m6t1] = loopdata(data_m6t1, l0_m6t1);
33
34 data_m6t2 = load(' /Users/merelmastenbroek/Allemaal Bestanden/
    BME/Afstuderen/Data-files/Data/21 02 19 13 52 16 muscle6-
    test2-2.txt ');
35 l0_m6t2 = 90;
36 [xaxis_m6t2, mean_F_m6t2, lmin_lmax_gemF_m6t2, L_op_Fmax,
    Fmax, contraction_m6t2] = loopdata(data_m6t2, l0_m6t2);
37
38 data_m6t3 = load(' /Users/merelmastenbroek/Allemaal Bestanden/
    BME/Afstuderen/Data-files/Data/21 02 19 13 59 02 muscle6-
    test3.txt ');
39 l0_m6t3 = 90;
40 [xaxis_m6t3, mean_F_m6t3, lmin_lmax_gemF_m6t3, L_op_Fmax,
    Fmax, contraction_m6t3] = loopdata(data_m6t3, l0_m6t3);
41
42 Gem_F_m6 = ((mean_F_m6t1 + mean_F_m6t3 + mean_F_m6t2)./3);
43
44 Fmax_90 = Fmax
45 %% l0 = 100mm
46 data_m3t1 = load(' /Users/merelmastenbroek/Allemaal Bestanden/
    BME/Afstuderen/Data-files/Data/21 02 18 12 05 50 muscle3-
    test1.txt ');
47 l0_m3t1 = 100;
48 [xaxis_m3t1, mean_F_m3t1, lmin_lmax_gemF_m3t1, L_op_Fmax,
    Fmax, contraction_m3t1] = loopdata(data_m3t1, l0_m3t1);
49
50 data_m3t2 = load(' /Users/merelmastenbroek/Allemaal Bestanden/
    BME/Afstuderen/Data-files/Data/21 02 18 12 16 29 muscle3-
    test2.txt ');
51 l0_m3t2 = 100;
52 [xaxis_m3t2, mean_F_m3t2, lmin_lmax_gemF_m3t2, L_op_Fmax,
    Fmax, contraction_m3t2] = loopdata(data_m3t2, l0_m3t2);
53

```



```
54 data_m3t5 = load(' /Users/merelmastenbroek/Allemaal Bestanden/  
    BME/Afstuderen/Data-files/Data/21 02 23 16 55 04 muscle3-  
    test5-2.txt ');  
55 l0_m3t5 = 100;  
56 [xaxis_m3t5, mean_F_m3t5, lmin_lmax_gemF_m3t5, L_op_Fmax,  
    Fmax, contraction_m3t5] = loopdata(data_m3t5, l0_m3t5);  
57  
58 Gem_F_m3 = ((mean_F_m3t5 + mean_F_m3t2 + mean_F_m3t1) ./ 3);  
59  
60 Fmax_100 = Fmax  
61 %% l0 = 110mm  
62 data_m5t2 = load(' /Users/merelmastenbroek/Allemaal Bestanden/  
    BME/Afstuderen/Data-files/Data/21 02 18 15 09 51 muscle5-  
    test2.txt ');  
63 l0_m5t2 = 110;  
64 [xaxis_m5t2, mean_F_m5t2, lmin_lmax_gemF_m5t2, L_op_Fmax,  
    Fmax, contraction_m5t2] = loopdata(data_m5t2, l0_m5t2);  
65  
66 data_m5t4 = load(' /Users/merelmastenbroek/Allemaal Bestanden/  
    BME/Afstuderen/Data-files/Data/21 02 19 12 06 34 muscle5-  
    test4.txt ');  
67 l0_m5t4 = 110;  
68 [xaxis_m5t4, mean_F_m5t4, lmin_lmax_gemF_m5t4, L_op_Fmax,  
    Fmax, contraction_m5t4] = loopdata(data_m5t4, l0_m5t4);  
69  
70 data_m5t5 = load(' /Users/merelmastenbroek/Allemaal Bestanden/  
    BME/Afstuderen/Data-files/Data/21 02 19 12 12 19 muscle5-  
    test5.txt ');  
71 l0_m5t5 = 110;  
72 [xaxis_m5t5, mean_F_m5t5, lmin_lmax_gemF_m5t5, L_op_Fmax,  
    Fmax, contraction_m5t5] = loopdata(data_m5t5, l0_m5t5);  
73  
74 Gem_F_m5 = ((mean_F_m5t5 + mean_F_m5t4 + mean_F_m5t2) ./ 3);  
75 Fmax_110 = Fmax  
76  
77 %% l0 = 120mm  
78  
79 data_m4t1 = load(' /Users/merelmastenbroek/Allemaal Bestanden/  
    BME/Afstuderen/Data-files/Data/21 02 18 13 29 46 muscle4-  
    test1.txt ');  
80 l0_m4t1 = 120;  
81 [xaxis_m4t1, mean_F_m4t1, lmin_lmax_gemF_m4t1, L_op_Fmax,  
    Fmax, contraction_m4t1] = loopdata(data_m4t1, l0_m4t1);  
82  
83 data_m4t3 = load(' /Users/merelmastenbroek/Allemaal Bestanden/  
    BME/Afstuderen/Data-files/Data/21 02 18 13 48 04 muscle4-  
    test3.txt ');  
84 l0_m4t3 = 120;  
85 [xaxis_m4t3, mean_F_m4t3, lmin_lmax_gemF_m4t3, L_op_Fmax,
```



```

    Fmax, contraction_m4t3] = loopdata(data_m4t3, l0_m4t3);
86
87 Gem_F_m4 = ((mean_F_m4t1 + mean_F_m4t3)./2);
88 Fmax_120 = Fmax
89 %% creating figures
90 newcolors = [0.83 0.14 0.14
91              1.00 0.54 0.00
92              0.47 0.25 0.80
93              0.25 0.80 0.54
94              0.25 0.25 0.90];
95
96 colororder(newcolors)
97
98 figure(1)
99 plot(contraction_m7t3, Gem_F_m7, '-o', 'linewidth', 2); hold
   on;
100 plot(contraction_m6t1, Gem_F_m6, '-o', 'linewidth', 2); hold
   on;
101 plot(contraction_m3t1, Gem_F_m3, '-o', 'linewidth', 2); hold
   on;
102 plot(contraction_m5t2, Gem_F_m5, '-o', 'linewidth', 2); hold
   on;
103 plot(contraction_m4t1, Gem_F_m4, '-o', 'linewidth', 2); hold
   on;
104
105 set(gca, 'FontSize', 16)
106 xlabel('Contraction of muscle [%]')
107 ylabel('Force [N]')
108 % legend('80', '80', '80', '90', '90', '90', '100', '100',
   '100', '110', '110', '110', '120', '120')
109 legend('80 mm', '90 mm', '100 mm', '110 mm', '120 mm')
110 title('Output force of pneumatic muscles (different L_0)')
111
112 figure(2)
113 % subplot(2,1,1)
114 % plot(xaxis_m7t3, mean_F_m7t3, 'r-o'); hold on;
115 % plot(xaxis_m7t2, mean_F_m7t2, 'r-*'); hold on;
116 % plot(xaxis_m7t1, mean_F_m7t1, 'r.-'); hold on;
117 % plot(xaxis_m6t1, mean_F_m6t1, 'k-o'); hold on;
118 % plot(xaxis_m6t2, mean_F_m6t2, 'k-*'); hold on;
119 % plot(xaxis_m6t3, mean_F_m6t3, 'k.-'); hold on;
120 % plot(xaxis_m3t1, mean_F_m3t1, 'g-o'); hold on;
121 % plot(xaxis_m3t2, mean_F_m3t2, 'g-*'); hold on;
122 % plot(xaxis_m3t5, mean_F_m3t5, 'g.-'); hold on;
123 % plot(xaxis_m5t2, mean_F_m5t2, 'b-o'); hold on;
124 % plot(xaxis_m5t4, mean_F_m5t4, 'b-*'); hold on;
125 % plot(xaxis_m5t5, mean_F_m5t5, 'b.-'); hold on;
126 % plot(xaxis_m4t1, mean_F_m4t1, 'r-o'); hold on;
127 % plot(xaxis_m4t3, mean_F_m4t3, 'r-*'); hold on;

```



```

128 % xlim([0 120])
129 % xlabel('length of muscle [mm]')
130 % ylabel('Force [N]')
131 % legend('80 muscle 7', '80', '80', '90 muscle 6', '90',
          '90', '100 muscle 3', '100', '100', '110 muscle5', '110',
          '110', '120 muscle 4', '120')
132 % set(legend, 'location', 'best')
133
134 newcolors = [0.83 0.14 0.14
135              1.00 0.54 0.00
136              0.47 0.25 0.80
137              0.25 0.80 0.54
138              0.25 0.25 0.90];
139
140 colororder(newcolors)
141
142 % subplot(2,1,2)
143 plot(xaxis_m7t3, Gem_F_m7, '-o', 'linewidth', 2); hold on;
144 plot(xaxis_m6t1, Gem_F_m6, '-o', 'linewidth', 2); hold on;
145 plot(xaxis_m3t5, Gem_F_m3, '-o', 'linewidth', 2); hold on;
146 plot(xaxis_m5t5, Gem_F_m5, '-o', 'linewidth', 2); hold on;
147 plot(xaxis_m4t1, Gem_F_m4, '-o', 'linewidth', 2); hold on;
148 set(gca, 'FontSize', 16)
149 title('Output force of pneumatic muscles (different L_0)')
150 legend('80 mm', '90 mm', '100 mm', '110 mm', '120 mm')
151 xlabel('Length of muscle [mm]')
152 ylabel('Force [N]')
153 set(legend, 'location', 'best')

```


C.2. Function "loopdata"

```

1  function [xaxis, mean_F, lmin_lmax_gemF, L_op_fmax, Fmax,
    contraction] = loopdata(data, l0)
2
3  time = data(:,1);           % time [ms]
4  time_s = time./1000;       % time [s]
5  V_force = data(:,2);       % Force [V]
6  V_distance = data(:,3);    % distance [V]
7  p_measured = data(:,4);    % measured pressure [bar]
8  p_atmosphere = 1.01325;    % atmospheric pressure [bar]
9  pressure = p_measured;     % pressure of muscle [bar];
10 force = data(:,5);         % Force [N]
11 distance = data(:,6);      % Distance [mm]
12 distance_cm = distance./10; % Distance [cm]
13 l0 = l0-5;                 % first 5mm were lost due to
    initial blowing up of the balloon
14
15 % create empty vectors
16 mean_F = [];
17 xaxis = [];
18 std_force = [];
19 contraction = [];
20
21 for i = 1:7
22     length_min = (l0-31)+(5*i-5);
23     length_max = (l0-29)+(5*i-5);
24     length = ((length_min+length_max)/2);
25     xaxis = [xaxis; length];
26     ind = find(distance >= length_min & distance < length_max
    );
27
28     F_ind = maxk(force(ind), 20);           % take 20
    indices when force is highest
29     gem_F = mean(F_ind);                   % take
    the mean value
30     gem_F(isnan(gem_F)) = 0;               % when
    NaN set to zero
31     mean_F = [mean_F; gem_F];              % create
    vector of force
32
33     Fmax = max(force);                     % find
    maximum force
34     Fmax_ind = find(force == Fmax);        % find
    index of maximum force
35     L_op_fmax = distance(Fmax_ind);        % length
    when F is maximum
36     contraction_Fmax = ((l0-L_op_fmax)./l0)*100; %
    contraction percentage when F is max

```



```
37
38     contraction_perc = ((l0-length)./l0)*100;           %
39         contraction percentage
40     contraction = [contraction; contraction_perc]; % create
41         vector of contraction percentage
42
43     std_F = std(F_ind);                                   %
44         standard deviation
45     std_force = [std_force; std_F];                     % create
46         vector of standard deviation
47
48     lmin_lmax_gemF(i,:) = [length_min length_max gem_F]; %
49         create vector of steps of length of muscle
50     i=i+1;
51 end
52
53 % create vectors including the last maximum values
54 xaxis = [xaxis; L_op_fmax];
55 mean_F = [mean_F; Fmax];
56 contraction = [contraction; contraction_Fmax];
57
58 end
```


C.3. Script mechanical tests muscle Pressure

```

1  clear all;
2  clc;
3  close all;
4
5  % Script thesis Merel Mastenbroek
6  % 06-04-2021
7  % Calculating pressure-length and pressure-contraction
   relationship of PAMs
8
9  %% L0 = 80mm
10 % load data
11 data_74 = load('Users/merelmastenbroek/Allemaal Bestanden/
   BME/Afstuderen/Data-files/Data/21 02 23 14 32 01 muscle7-
   test4.txt');
12
13 % define L0 of the muscle
14 L0_74 = 80;
15
16 % calculate pressure at 15N of the muscle using the function
   'pressure15N'
17 [xaxis_74, mean_p_74, f_ind_74, contraction_74] = pressure15N
   (data_74, L0_74);
18
19 %% L0 = 90mm
20 data_64 = load('Users/merelmastenbroek/Allemaal Bestanden/
   BME/Afstuderen/Data-files/Data/21 02 19 14 05 43 muscle6-
   test4.txt');
21 L0_64 = 90;
22 [xaxis_64, mean_p_64, f_ind_64, contraction_64] = pressure15N
   (data_64, L0_64);
23
24 %% L0 = 100mm
25 data_39 = load('Users/merelmastenbroek/Allemaal Bestanden/
   BME/Afstuderen/Data-files/Data/21 02 23 17 17 29 muscle3-
   test9.txt');
26 L0_39 = 100;
27 [xaxis_39, mean_p_39, f_ind_39, contraction_39] = pressure15N
   (data_39, L0_39);
28
29 %% L0 = 110mm
30 data_53 = load('Users/merelmastenbroek/Allemaal Bestanden/
   BME/Afstuderen/Data-files/Data/21 02 18 15 14 07 muscle5-
   test3-2.txt');
31 L0_53 = 110;
32 [xaxis_53, mean_p_53, f_ind_53, contraction_53] = pressure15N
   (data_53, L0_53);
33

```



```

34 %% L0 = 120mm
35 data_42 = load( '/Users/merelmastenbroek/Allemaal Bestanden/
    BME/Afstuderen/Data-files/Data/21 02 18 13 36 33 muscle4-
    test2.txt' );
36 L0_42 = 120;
37 [xaxis_42, mean_p_42, f_ind_42, contraction_42] = pressure15N
    (data_42, L0_42);
38
39 %% creating figures
40
41 newcolors = [0.83 0.14 0.14
42              1.00 0.54 0.00
43              0.47 0.25 0.80
44              0.25 0.80 0.54
45              0.25 0.25 0.90];
46
47 colororder(newcolors)
48
49 figure(1)
50 subplot(2,1,1)
51 plot(xaxis_74, mean_p_74, '-o', 'linewidth', 2); hold on
52 plot(xaxis_64, mean_p_64, '-o', 'linewidth', 2); hold on
53 plot(xaxis_39, mean_p_39, '-o', 'linewidth', 2); hold on
54 plot(xaxis_53, mean_p_53, '-o', 'linewidth', 2); hold on
55 plot(xaxis_42, mean_p_42, '-o', 'linewidth', 2); hold on
56 set(gca, 'FontSize', 16)
57 xlabel('length [mm]')
58 ylabel('pressure [bar]')
59 legend('80 mm', '90 mm', '100 mm', '110 mm', '120 mm')
60 set(legend, 'location', 'best')
61 title('Pressure to reach output force of 15N')
62
63 newcolors = [0.83 0.14 0.14
64              1.00 0.54 0.00
65              0.47 0.25 0.80
66              0.25 0.80 0.54
67              0.25 0.25 0.90];
68
69 colororder(newcolors)
70 subplot(2,1,2)
71 plot(contraction_74, mean_p_74, '-o', 'linewidth', 2); hold
    on
72 plot(contraction_64, mean_p_64, '-o', 'linewidth', 2); hold
    on
73 plot(contraction_39, mean_p_39, '-o', 'linewidth', 2); hold
    on
74 plot(contraction_53, mean_p_53, '-o', 'linewidth', 2); hold
    on
75 plot(contraction_42, mean_p_42, '-o', 'linewidth', 2); hold

```



```
    on
76  set(gca, 'FontSize', 16)
77  xlabel('contraction [%]')
78  ylabel('pressure [bar]')
79  legend('80 mm', '90 mm', '100 mm', '110 mm', '120 mm')
80  set(legend, 'location', 'best')
```


C.4. Function "pressure15N"

```

1  function [xaxis, mean_p, F_index, contraction] = pressure15N(
    data, l0)
2
3  time = data(:,1);           % time [ms]
4  time_s = time./1000;       % time [s]
5  V_force = data(:,2);       % Force [V]
6  V_distance = data(:,3);    % distance [V]
7  p_measured = data(:,4);    % measured pressure [bar]
8  p_atmosphere = 1.01325;    % atmospheric pressure [bar]
9  pressure = p_measured - p_atmosphere; % pressure of
    muscle [bar];
10 force = data(:,5);         % Force [N]
11 distance = data(:,6);      % Distance [mm]
12 distance_cm = distance./10; % Distance [cm]
13 % create empty vectors
14 mean_p = [];
15 xaxis = [];
16 F_index = [];
17 contraction = [];
18 for i = 1:7 % 7 steps
19     length_min = (l0-31)+(5*i-5); % every step length
        decreases 5mm from L0
20     length_max = (l0-29)+(5*i-5);
21     length = ((length_min+length_max)/2);
22     xaxis = [xaxis; length];
23
24 ind = find((distance >= length_min & distance < length_max) &
    (force >= 14.8 & force <= 15.3)); %find indices where
    distance was between a certainvalue and force was between
    14.8 and 15.3N
25     f_ind = force(ind);      % force value at those
        indices
26     p_ind = maxk(pressure(ind), 20); % pressure value
27     gem_p = mean(p_ind);     % mean pressure
28     mean_p = [mean_p; gem_p]; % create vector of mean
        pressure
29     F_index = [F_index; f_ind]; % create vector of force
        values
30
31     contraction_perc = ((l0-length)./l0)*100; %
        contraction percentage
32     contraction = [contraction; contraction_perc]; % create
        vector of contraction percentage
33     i = i+1;
34 end

```


C.5. Stringpot vs laser

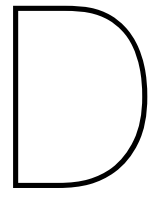
```

1 clear all;
2 clc;
3 close all;
4
5 % Script thesis Merel Mastenbroek
6 % 06-04-2021
7
8 %%
9 % load data laser
10 data = load('/Users/merelmastenbroek/Allemaal Bestanden/BME/
    Afstuderen/Data-files/21_02_19_16_13_06_stringpot3.txt');
11 data2 = load('/Users/merelmastenbroek/Allemaal Bestanden/BME/
    Afstuderen/Data-files/21_02_19_16_08_13_stringpot2.txt');
12 laser = data(:,6); % distance values measured by the
    laser test 1 and 2
13 laser3 = data2(:,6); % distance values measured by the
    laser test 3
14 laser3 = laser3(1:5:end); % adjusted for sample time of
    laser, 5x higher compared to stringpot.
15
16 % load data stringpot
17 Pot = load('/Users/merelmastenbroek/Allemaal Bestanden/BME/
    Afstuderen/pot-test1.txt');
18 Pot2 = load('/Users/merelmastenbroek/Allemaal Bestanden/BME/
    Afstuderen/pot-test2.txt');
19
20 % create vectors (start time end end time of test)
21 %test 1
22 pot_1 = Pot(1:106);
23 laser_1 = laser(476:581);
24 %test 2
25 pot_2 = Pot(223:375);
26 laser_2 = laser(698:850);
27 %test 3
28 pot_3 = Pot2(10:49);
29 laser_3 = laser3(83:122);
30
31 % calculate difference between laser and stringpot
32 diff_1 = laser_1 - pot_1;
33 diff_2 = laser_2 - pot_2;
34 diff_3 = laser_3 - pot_3;
35
36 %% Create figures
37 figure(1)
38 subplot(3,1,1)
39 plot(pot_1, 'linewidth', 2)
40 hold on;

```



```
41 plot(laser_1, 'linewidth', 2)
42 set(gca, 'FontSize', 12)
43 ylabel('distance [mm]')
44 title('Distance measurement laser and stringpot test 1')
45 legend('Stringpot', 'Laser')
46 set(legend, 'location', 'best')
47
48 subplot(3,1,2)
49 plot(pot_2, 'linewidth', 2)
50 hold on;
51 plot(laser_2, 'linewidth', 2)
52 set(gca, 'FontSize', 12)
53 ylabel('distance [mm]')
54 title('Distance measurement laser and stringpot test 2')
55 legend('Stringpot', 'Laser')
56 set(legend, 'location', 'best')
57
58 subplot(3,1,3)
59 plot(pot_3, 'linewidth', 2)
60 hold on;
61 plot(laser_3, 'linewidth', 2)
62 set(gca, 'FontSize', 12)
63 ylabel('distance [mm]')
64 title('Distance measurement laser and stringpot test 3')
65 legend('Stringpot', 'Laser')
66 set(legend, 'location', 'best')
67 ylim([0 65])
68
69 % set values into groups for boxplots
70 v_diff = [diff_1; diff_2; diff_3];
71 grp = [zeros(1, length(diff_1)), ones(1, (length(diff_2))), 2*
       ones(1, (length(diff_3)))];
72
73 % boxplot difference
74 figure(2)
75 h = boxplot(v_diff, grp, 'Labels', {'Test 1', 'Test 2', 'Test 3'});
76 set(h, {'linewidth'}, {1.5})
77 title('Boxplot of difference in distance laser – stringpot')
78 ylim([-3 4.5])
79 set(gca, 'FontSize', 16)
80 ylabel('difference in distance [mm]')
```

SOLIDWORKS Drawings

4

3

2

1

F

F

E

E

D

D

C

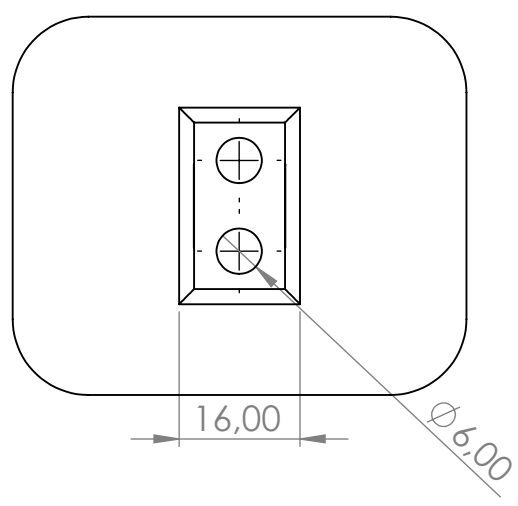
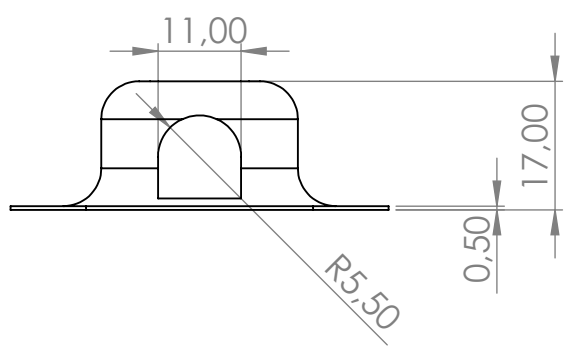
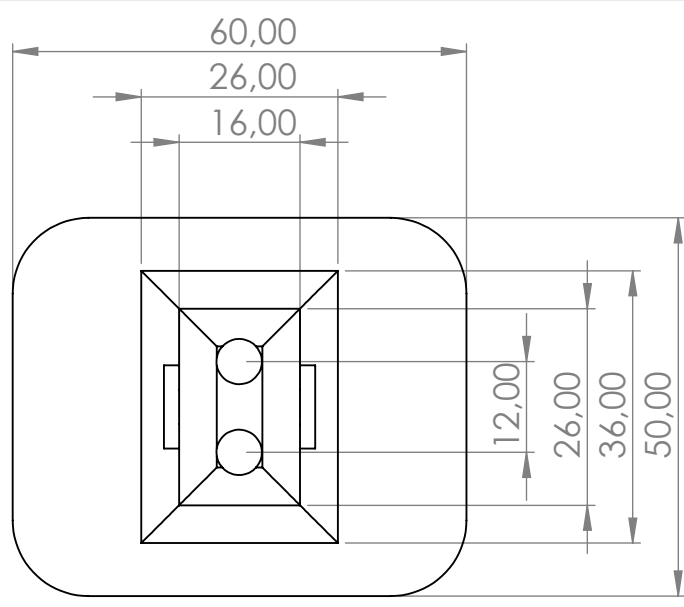
C


B

B

A

A



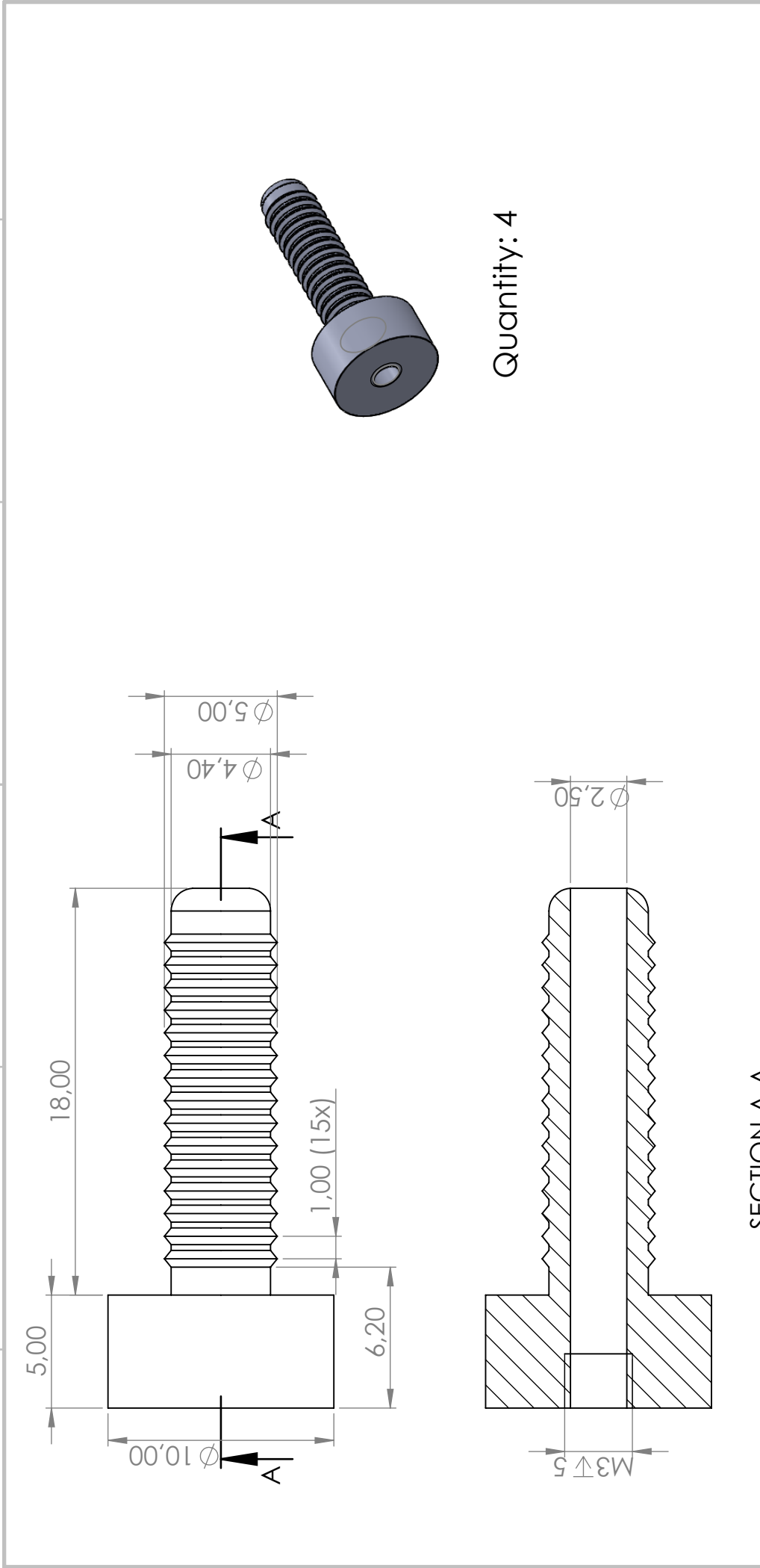
<p>UNLESS OTHERWISE SPECIFIED: DIMENSIONS ARE IN MILLIMETERS SURFACE FINISH: TOLERANCES: LINEAR: ANGULAR:</p>				<p>FINISH:</p> 		<p>DEBURR AND BREAK SHARP EDGES</p>		<p>DO NOT SCALE DRAWING</p>		<p>REVISION</p>																							
<table border="1"><thead><tr><th></th><th>NAME</th><th>SIGNATURE</th><th>DATE</th></tr></thead><tbody><tr><td>DRAWN</td><td></td><td></td><td></td></tr><tr><td>CHK'D</td><td></td><td></td><td></td></tr><tr><td>APPV'D</td><td></td><td></td><td></td></tr><tr><td>MFG</td><td></td><td></td><td></td></tr><tr><td>Q.A</td><td></td><td></td><td></td></tr></tbody></table>					NAME	SIGNATURE	DATE	DRAWN				CHK'D				APPV'D				MFG				Q.A				<p>TITLE:</p>		<p>DWG NO.</p> <p>sticker-drawing</p>		<p>A4</p>	
					NAME	SIGNATURE	DATE																										
				DRAWN																													
				CHK'D																													
				APPV'D																													
				MFG																													
Q.A																																	
				<p>MATERIAL:</p> <p>MPFlex</p>																													
				<p>WEIGHT:</p>		<p>SCALE:1:1</p>		<p>SHEET 1 OF 1</p>																									

4

3

2

1



Quantity: 4

SECTION A-A
SCALE 4 : 1

UNLESS OTHERWISE SPECIFIED: DIMENSIONS ARE IN MILLIMETERS		FINISH:		TU Delft		DEBURE AND BREAK SHARP EDGES		DO NOT SCALE DRAWING		REVISION	
SURFACE FINISH:		TOLERANCES:		DATE		08-12-2020		Merel Mastenbroek (4723333)		TITLE:	
LINEAR:		SIGNATURE		MATERIAL:		Aluminium		begin part PAM v2		DWG NO.	
ANGULAR:		NAME		Q.A		drawing-begin-v2		A4		SCALE:2:1	
DRAWN		DATE		WEIGHT:		SHEET 1 OF 1					
CHK'D											
APP'VD											
MFG											
Q.A											

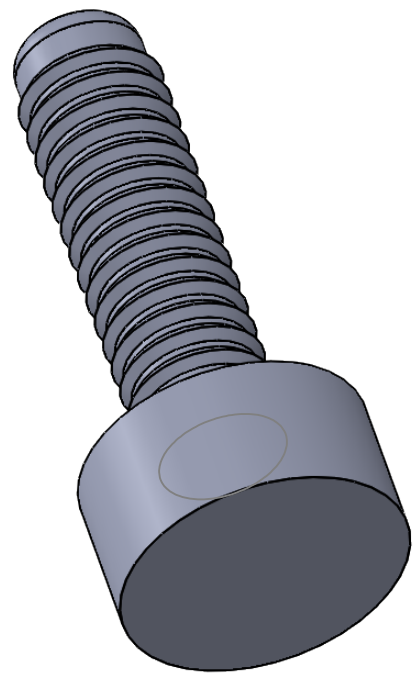
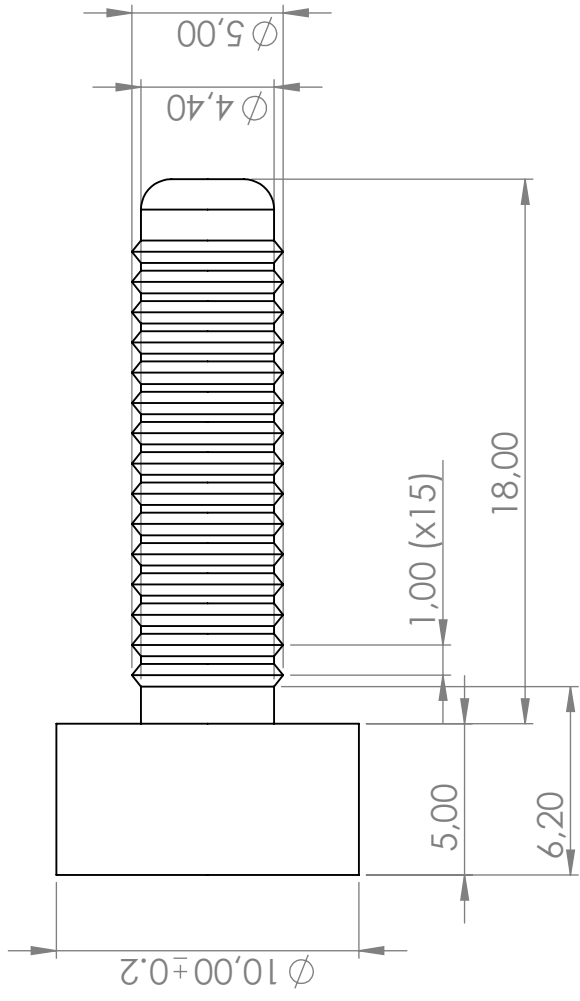
6 5 4 3 2 1

D

C

B

A



Quantity: 4

UNLESS OTHERWISE SPECIFIED: DIMENSIONS ARE IN MILLIMETERS		FINISH:		TU Delft		DEBURE AND BREAK SHARP EDGES		DO NOT SCALE DRAWING		REVISION	
SURFACE FINISH:		TOLERANCES:		DATE		TITLE:		Merel Mastenbroek (4723333)			
LINEAR:		ANGULAR:		SIGNATURE		08-12-2020		End part PAM version 2			
DRAWN											
CHK'D											
APP'VD								Quantity: 4			
MFG								DWG NO. A4			
Q.A								drawing-end-v2			
								SCALE:2:1			
								SHEET 1 OF 1			

4

3

2

1

F

F

E

E

D

D

C

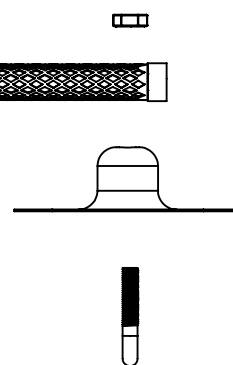
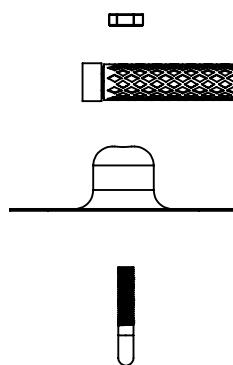
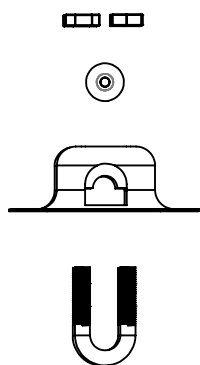
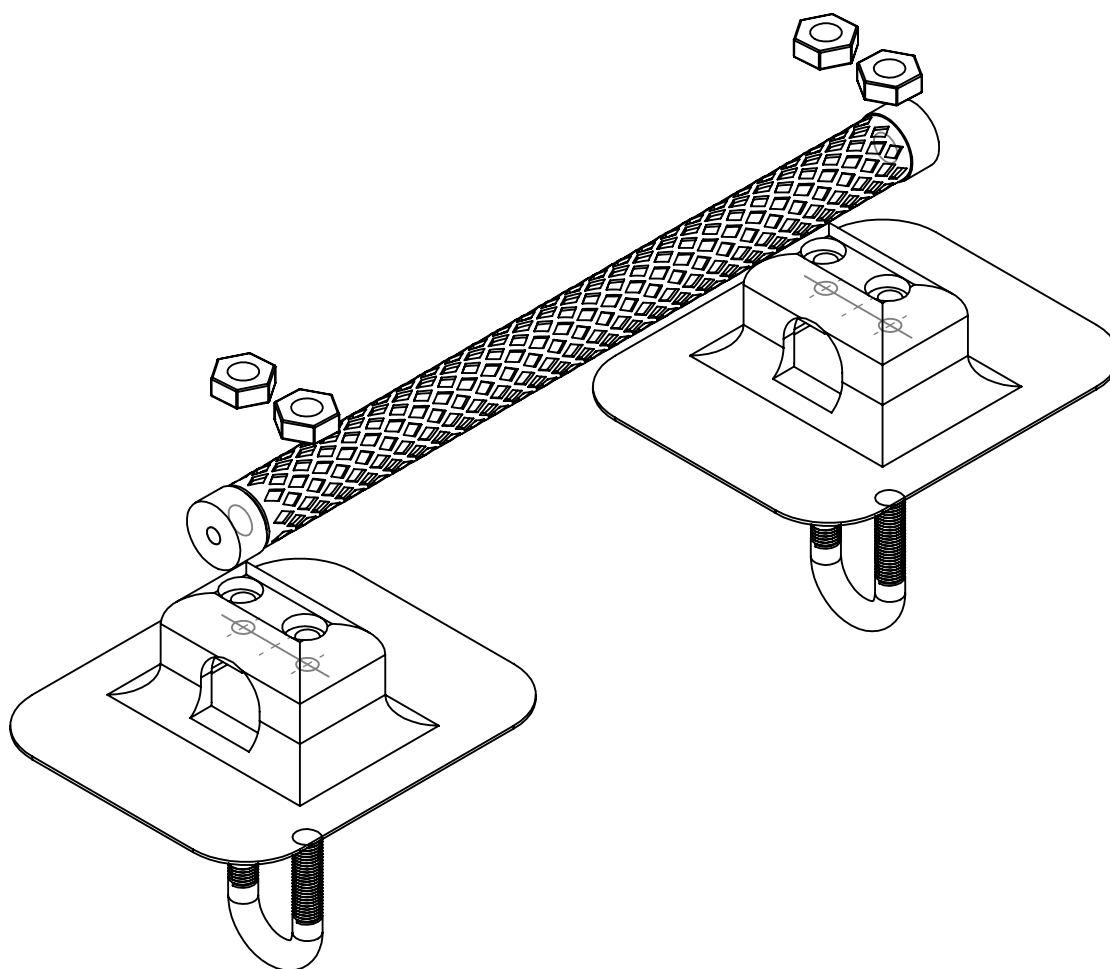
C

B

B

A

A



UNLESS OTHERWISE SPECIFIED:
DIMENSIONS ARE IN MILLIMETERS
SURFACE FINISH:
TOLERANCES:
LINEAR:
ANGULAR:

FINISH:



DEBURR AND
BREAK SHARP
EDGES

DO NOT SCALE DRAWING

REVISION

	NAME	SIGNATURE	DATE		
DRAWN					
CHK'D					
APPV'D					
MFG					
Q.A					

MATERIAL:

WEIGHT:

TITLE:

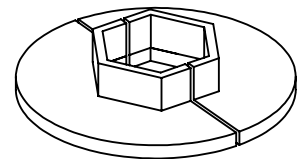
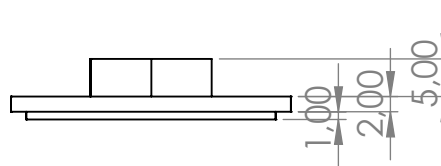
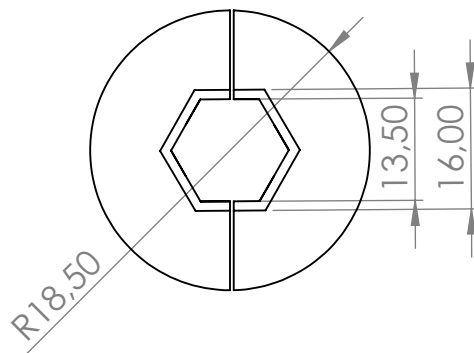
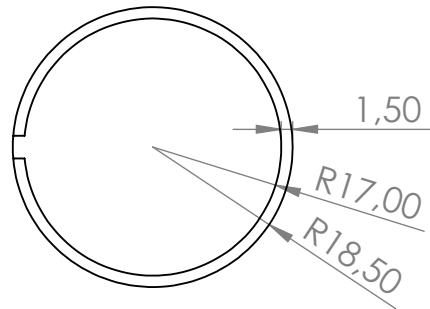
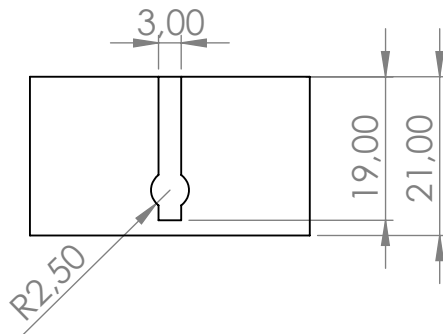
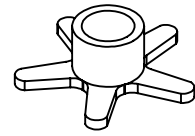
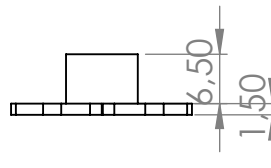
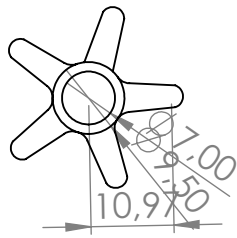
DWG NO.


Total-assembly

A4

SCALE:1:2

SHEET 1 OF 1



UNLESS OTHERWISE SPECIFIED: DIMENSIONS ARE IN MILLIMETERS SURFACE FINISH: TOLERANCES: LINEAR: ANGULAR:			FINISH: 		DEBURR AND BREAK SHARP EDGES		DO NOT SCALE DRAWING		REVISION		
							TITLE:				
DRAWN								DWG NO. <div>Parts-drawing</div>			
CHK'D											
APPV'D											
MFG											
Q.A											
				MATERIAL: <div>PLA tough black</div>				A4			
				WEIGHT:				SCALE:2:1			
								SHEET 1 OF 1			

